IMMUNE RESPONSE TO SYNTHESIZED PNIPAM-BASED GRAFT HYDROGELS

IMMUNE RESPONSE TO SYNTHESIZED PNIPAM-BASED GRAFT HYDROGELS CONTAINING CHITOSAN AND HYALURONIC ACID

By

MARIAM D. AL-HAYDARI, B.Sc., B.A.

A Thesis

Submitted to the School of Graduate Studies

in Partial Fulfillment of the Requirements

for the Degree

Master of Applied Science, Chemical Engineering

McMaster University

MASTER OF APPLIED SCIENCE (2010) McMaster University

(Chemical Engineering) Hamilton, Ontario

TITLE: Immune Response to Synthesized Pnipam-Based Graft Hydrogels Containing Chitosan and Hyaluronic Acid

AUTHOR: Mariam D. Al-Haydari, B.Sc., B.A.

SUPERVISOR: Dr. K. Jones

NUMBER OF PAGES: xii, 108

Abstract

Biomaterials are thought to be the magical solution to improving the quality of life and lengthening lifespans of human beings. To date, there is no biomaterial that can completely escape immune responses. However, successes have recently been made in reducing immune responses to biomaterials.P(N-isopropylacrylamide) (PNIPAM), chitosan , and hyaluronan are examples of polymers that are gaining great interest in the field of biomaterials. The most attractive property of PNIPAM is thermo-responsiveness. Adequate literature has been published on improving the mechanical strength of PNIPAM, but not much has been published on host response to PNIPAM based graft-polymers. Chitosan and hyaluronan are generally considered non-toxic and non-immunogenic.

The first part of this project focuses on the synthesis and characterization of hyaluronan-grafted-chitosan-grafted-P(NIPAM-co-acrylic acid), while the second part examines the effect of grafting on the extent of immune reaction compared to P(NIPAM-co-acrylic acid) alone. The incorporation of chitosan into P(NIPAM-co-acrylic acid), and hyaluronan into chitosan-grafted-P(NIPAM-co-acrylic acid) was confirmed by Fourier Transform Infrared Spectroscopy, Nuclear Magnetic Resonance , 2,4,6-trinitrobenzenesulfonic acid (TNBS), and Lower Critical Solution Temperature (LCST) experiments. The optimum molecular weight for P(NIPAM-co-acrylic acid) that could provide sufficient amount of

reactive sites while maintaining LCST below 37 °C was found to be in the range of 2-2.5kDa. Western blotting results demonstrated that incorporating chitosan into P(NIPAM-co-acrylic acid) reduces the amount of fibrinogen, fibronectin, and vitronectin adsorbed, and eliminates complement component 3 (C3) adsorption.

Furthermore, incorporating hyaluronan eliminates more inflammatory proteins including fibrinogen and reduces Immunoglobulin G (IgG) adsorption. Chitosan-grafted-P(NIPAM-co-acrylic acid) elicited lower levels of inflammatory cytokine release compared to P(NIPAM-co-acrylic acid), but higher than hyaluronan-grafted-chitsan-grafted-P(NIPAM-co-acrylic). *In vitro* and *in vivo* results revealed lowest density of leukocytes adhesion to hyaluronan containing surface compared to the other surfaces. The extent and duration of inflammation was reduced on chitosan-grafted-P(NIPAM-co-acrylic acid) and hyaluronan-grafted-chitosan-grafted-P(NIPAM-co-acrylic acid) hydrogels.

Acknowledgements

Despite the challenging and stressful nature of independent research, learning about biomaterials and tissue engineering has been very pleasant. I thank you Dr. Jones for allowing me to freely choose my thesis project and having trust in me. I thank you for being easygoing, respectful, and humourous.

My heartfelt thanks to Dr. Brash and his graduate students. Special thanks to Kyla Sask and Sara Alibeik for their help and wonderful manners. I am very grateful to Paulina Kowalewska and Mandy Patrick's support and help with *in vivo* work. Their kindness has made my life as a graduate student a lot easier. I would like to also express my gratitude to Dr. Sheardown and her research group for the great advice and for being warm lab neighbours. Dr. Pelton, thank you for allowing me to use your lab equipment. Last but not least, Dr. Haure disserves special recognition for his kindness and willingness to help. I took advantage of his kindness and considered myself an extended member of his group.

I would like to thank my research colleagues, Ryan Love and Jen Solaimani, for their friendship and support. The help of undergraduate student Ryan McBride saved me one month of exhausting work. My friendships with Salma Falah Toosi and Vajiheh Akbarzadeh made my most joyful memories at McMaster University.

This acknowledgement section would not be complete if I did not mention

my undergraduate research experience at Wayne State University in Michigan. If it was not for the research experience that I gained in the da Rocha group, it would not have been possible for me to accomplish what I have accomplished. I thank Dr. Sandro da Rocha for giving me the opportunity to work with his research group and for his invaluable guidance. I also thank Balaji Bharatwaj for his endless help and friendship and Libu Wu for being a great model of hard work.

Finally, I would like to dedicate this work to the most important people in my life, my husband and my family. Your presence in my life, along with your love, support and friendship, is such a blessing. You have always empowered me to live in the right way, and be happy and strong.

Table of Contents

List of Figures

List of Tables

1. Introduction

The success of tissue engineering, gene therapy, and drug delivery system is only possible with the advancement of biomaterials research [1-6]. Biomaterials are the central elements of biomedical devices and serve two main roles: making up the device; and, determining its performance. The performance of biomaterials depends not only on their mechanical, physical, chemical, and biological properties, but also on the extent of induced nonspecific immune reactions [1, 3, 7-9]. Biological interaction, including immune responses, at the interface of biomaterials is mediated by adsorbed proteins [1, 7, 8, 10, 11]. The complexity of proteins' structures and the inability to control protein adsorption led biomaterials researchers to examine protein resistant, non-fouling, surfaces [1, 7, 12].

PEG-coating has been shown to prompt the resistance of surface proteins. Two factors contribute to the non-fouling property of PEG: the tendency of the PEG chain to retain the volume of random coil; and, the tendency of the PEG chain to resist the release of bound water molecules [7, 13]. Hence, the hydrophilicity and the ability to retain large amounts of water are important characteristics of biomaterials, and it is these characteristics that have rendered hydrogels an important class of biomaterials [1, 7, 12, 14, 15].

Hyaluronic acid (HA) is a very extensively studied hydrogel due to its biocompatibility, unique viscoelastic properties, high permeability, high water

content, and physical properties [16]. In addition to controlled drug delivery systems, HA has shown a potential in various tissue engineering applications, such as soft tissue augmentation, articular cartilage regeneration, artificial skin, facial intradermal implants, and wound healing [14]. HA is a naturally occurring polysaccharide composed of alternating N-acetyl-β-D-glucosamime and β-D-glucuronic acid units. HA is a major constituent of the extracellular matrix (ECM) serving mechanical, rheological, and biological functions [5].

Three groups of HA-specific receptors that mediate interactions with HA have been identified on various cells, including leukocytes: CD44; receptor for HA-mediated motility (RHAMM); and, intracellular adhesion molecule-1 (ICAM-1). These receptors are responsible for mediating various physiological events, such as cell aggregation, migration, proliferation, and activation [16, 17]. Studies have demonstrated that the binding of cell receptors to HA is dependent on the extent of crosslinking [16-18].

Crosslinking is also effective in increasing the half-life of HA in the tissue. Megan S. Lord *et al* have demonstrated that HA enzymatic degradation was markedly reduced by grafting to poly(N-Isopropylacrylamide) (PNIPAM) [18]. Incorporating HA into PNIPAM not only improves cell adhesion and degradation rate, but also adds *in situ* gelling features because of the thermoresponsive character of PNIPAM. *In situ* temperature-based gelling is useful for injectable applications with advantages ranging from ease of application, localization, non-invasiveness, and patient comfort [19].

PNIPAM is a non-degradable synthetic polymer that exhibits a lower critical solution temperature (LCST) in a range comparable to body temperature [12, 20, 21]. The reactivity as well as the LCST of PNIPAM could be altered by controlling the length of the polymer, introducing co-monomer or graft polymer, or by proper selection of transfer agent [12, 22]. The poor biocompatibility and mechanical properties of PNIPAM can be improved by incorporating biocompatible polymers with higher mechanical strength. HA-grafted-chitosan-grafted-PNIPAM, HA-g-CS-g-P(NIPAM), has a great potential as an injectable biomaterial for tissue engineering, drug delivery, and gene therapy applications [23-25].

In this work, we have selected P(NIPAM-co-acrylic acid), P(NIPAM-co-AA), as a base copolymer to which chitosan and HA were grafted. The effects of molecular weight, AA content, and graft ratio on the sol-gel behaviour of the polymer were examined. Protein adsorption, *in vitro*, and *in vivo* evaluation of immune responses were evaluated.

2. Background

2.1. Biomaterials

Drug delivery systems, gene therapy, and tissue engineering are some of the most fascinating outcomes of the collaboration between engineers, scientists, and physicians. The medical field is expected to witness revolutionary changes in treatment approaches and options with the rapid progress of research in drug delivery systems, gene therapy, and tissue engineering. Excellent drug delivery devices are being introduced with controlled release profile and/or targeted delivery [5, 7, 12, 26]. Such devices not only improve the therapeutic efficacy of the therapeutic agent, but also provide more ease and comfort to patients. Gene therapy provides alternative and new treatment options to a wide scope of diseases. Gene therapy's approach to curing or treating diseases is through employing functional genes to correct or replace cell function [27, 28]. Tissue engineering, a less advanced field, involves collaborative work between engineers and scientists to produce artificial tissues and organs.

In addition to active components such as gene codes, cells, and proteins, biomaterials are always involved in the design of drug delivery systems, gene therapy, and tissue engineered devices. Biomaterials are evaluated on a biocompatibility scale, which is device or application dependent [7, 14]. Biocompatibility is assessed based on the ability of a material to support device-

specific functions without triggering undesirable host responses [1, 8, 11]. The biggest challenge in biomaterials research is to design a biomaterial that is capable of accounting for the complexity of biological systems, manifested by the presence of various types of cells, biological components, processes, and physiological conditions, in directing only particular components of interest to perform a particular task of interest.

Periodontal scaffolds, for example, should be engineered in a way that supports osteoblast adhesion, migration, and proliferation, while inhibiting the migration of epithelial cells. The adhesion of chondrocytes on a cartilage implant is desirable, whereas the adhesion of leukocytes would lead to undesirable host reactions [1, 8, 11]. Except when employed as vaccine adjuvants, biomaterials should always escape immune responses. A great deal of knowledge in human physiology is needed to achieve such a goal. Utilizing specific physiological features makes it possible to trick physiological components to perform the desired task.

The types and characteristics of cellular-biomaterial interactions are known to be mediated by adsorbed proteins at the biomaterial surface [3, 8, 11]. Nonspecific proteins adsorb to biomaterials surfaces immediately post implantation. The complexity and heterogeneity of proteins accounts for their high and chemistry independent affinity to biomaterials surfaces. Protein adsorption to biomaterials surfaces is driven by electrostatic bonding, hydrogen bonding, van der Waals, and hydrophobic forces [7, 29]. The inability to prevent

nonspecific protein adsorption lead researchers to examine protein resistant, also known as "non-fouling", surfaces.

In vitro studies have shown that the interaction between cells and biomaterials is influenced by the biomaterial's chemical, physical, mechanical, and biological properties. Ceramics, metals, and polymers are the main classes of materials used for biomedical applications. The versatility of polymers renders them the most extensively used class of biomaterials. Polymers can be classified on the basis of degradation, natural or synthetic origin, and according to their physical or chemical properties.

A great deal of interest has been directed towards investigating hydrogels for biomedical applications. A hydrogel is a water-swollen polymer network that can hold a large amount of water while maintaining its three dimensional structure [7, 14, 16]. Hydrogels are generally nontoxic, protein resistant, structurally resemble biological macromolecules, and allow for easy transport of active components [18]. Hydrogels are widely employed in controlled release drug delivery devices.

2.1.1. Bulk/Surface Chemistry

Cells interact with the surface of a biomaterial via the rapidly absorbed protein monolayer. Achieving controlled cellular behaviour at the implant surface can be made possible by controlling the type of proteins adsorbed [30, 31]. *In*

vitro studies have demonstrated chemistry dependent protein adsorption. Proteins are adsorbed onto biomaterials via ionic, van der Waals, hydrophobic, and hydrogen forces. Since bulk chemistry has a direct effect on the physical and mechanical properties of the biomaterial, surface chemical modification is the best approach to controlling adsorbed proteins without affecting other properties.

Self-assembeled monolayers (SAMs) with different terminal functional groups allows for evaluating effects of different functional groups on host response. Barbosa *et al* evaluated the influence of COOH, OH, and CH_3 groups of SAMs on fibrous capsule formation and cell recruitment [32]. The group observed an increase in fibrous capsule thickness around CH_3-terminated SAMS and control cold surfaces, in comparison to sham-operated mice and COOH- and OH-covered SAMS. Table 2-1 lists the effects of different functional groups on cell response [9].

2.1.2. Physical Properties

Wettability is an important measure in biomedical applications. Hydrophobic surfaces are known to expel water, resulting in high and undesirable levels of protein adsorption followed by unfolding of protein with high entopic gain that leads to irreversible adsorption [33, 34]. On the other hand, hydrophilic surfaces absorb water. The resistance of hydrophilic surfaces to protein adsorption is favoured by entropy with the tendency of hydrophilic chains

to retain bound water. Hydrophilic – but not too hydrophilic – surfaces are beneficial from this perspective [7, 9, 30, 35].

Table 2-1: Effect of surface chemistry on cell responses.

Functional Group	Cells Studied	Type of Study
CH_3	Endothelial cells Human fibroblast cells Neutrophile cells Myoblast cells	Adhesion Adhesion Adhesion Proliferation and differentiation
OH	Osteoblast Mesenchymal stem cells	Adhesion Adhesion, proliferation, mRNA expression
NH_2	Endothelial cells Myoblast	Adhesion Proliferation and differentiation
COOH	Human fibroblast Myoblast	Adhesion Proliferation and differentiation
Phosphorylcholine	Neutrophils	Adhesion

Topography refers to discontinuity in a surface, whether in an organized fashion, such as in micro- or nano-textured surfaces, or in a disorganized fashion, such as in rough or porous surfaces [36]. Based on extensive research, it is clear that protein adsorption and cell behaviour are not only affected by the dimension of the physical topography, but also by geometric patterns. Geometric patterns include grooves, ridges, pillars, and dots. Topographical features control cell adsorption, denaturing, adhesion, morphology, orientation, migration,

proliferation and differentiation [9, 37, 38].

For example, fibers with diameters less than 5 μm inhibited foreign body reactions and no fibrous capsule was formed, while fibers with a diamters greater than 5 μm did not influence immune reactions [39]. It is suggested by many reports that introducing particular topographical features inhibits biomaterials immune recognition. Similarly, foreign body reactions associated with porous materials was significantly reduced when pore-size was 5-15 μm [40-43]. The response was independent of materials when pore-size were within this range.

2.2. Hydrogels

Hydrogels are an interesting class of biomaterials with a structure that resembles biological macromolecular components [14]. The ability of hydrogels to hold a large amount of water not only results in reduced protein adsorption, if not eliminated, but also provide porous polymeric network allowing for controllable permeability to biological or therapeutic solutes [7, 14, 44, 45]. Hydrogels can be classified according to their natural or synthetic origin, preparation method, ionic charge, and physical structure. Important criteria of hydrogels include swelling behaviour, mechanical properties, degradation kinetics and mechanism, and biocompatibility [7].

A great deal of research has been focused on hydrogels that exhibit

environment-sensitive gelation, such as pH- or temperature-sensitive gelation. pH-sensitive hydrogels are made of polyeletrolytes, which are polymers that exhibit a large number of ionisable acidic or basic pendent groups [7, 12, 15]. Pendent groups' ionization, in response to the appropriate pH and ionic strength, induce electrostatic repulsion forces that result in swelling of the polymer network. Poly(acrylic acid) and poly(N,N'-diethylaminoethyl methacrylate) become ionized at high, and low pH, respectively. Variations in physiological pH directed researchers to examine pH-sensitive hydrogels for controlled and targeted drug delivery applications. The critical point at which the swelling is observed can be altered to the desired application, which takes into account physiological aspects. For example, numerous pH-sensitive microparticles have been designed to deliver active components specifically to cytoplasm utilizing the burst effect of microparticles at a pH of 4.

Similarly, various methods have been utilized to design temperature sensitive hydrogels with a critical transition point close to physiological temperature (37 °C) [12, 14, 20, 24, 25]. Temperature-sensitive polymers undergo phase transition (sol-gel) in response to temperature increase. Unlike most polymers, thermoresponsive polymers immiscible in water at increased temperature. There is a critical point at which the transition occurs. Temperature-sensitive polymers are either moderately hydrophobic, or contain hydrophilic and hydrophobic moieties. Hydrogen bonding between the hydrophilic segments of polymer and water molecules dominates at room temperature. At higher

temperatures, hydrogen bonding weakens and hydrophobic interactions among hydrophobic segments dominate. The result is transition from random coil to compact globule conformation.

The point at which phase transition occurs is termed the lower critical solution temperature (LCST). LCST is dependent on hydrophilic to hydrophobic segments. A higher ratio of hydrophobic to hydrophilic segments decreases LCST, while a lower ratio increases LCST. In addition to polymer molecular weight, the ratio of hydrophobic to hydrophilic segments influences the critical gelation concentration (CGC) [20, 21]. Below CGC, the polymer precipitates in response to temperature increase. Above CGC, a non-flowing gel is formed. There are two types of temperature-sensitive transitions, sol-gel and swelling-shrinking transition. Hydrogels that are not made of covalently crosslinked polymers undergo a sol-gel phase transition instead of swelling shrinking transitions [12].

Natural and synthetic thermoresponsive hydrogels have been discovered. Examples of natural thermoresponsive polymers include gelatin (protein prepared from the partial hydrolysis of collagen) and polysacchardies such as agarose, amylopectin, cellulose derivatives, carrageenans, and Gellan [14, 21, 46]. Although natural polymers offer interesting advantages such as reduced toxicity, biological recognition, normal remodelling, some challenges are present in terms of their complex structure, unpredictable properties, strong immune response, and possibility of disease transmission [2, 47, 48]. Synthetic

thermoresponsive hydrogels, such as poly(N-isopropylacryl amide), poly(N,N-diethylacrylamide), PEO/PPO block copolymers, and PEG/PLGA block copolymers, do not offer ideal alternatives due to their week mechanical properties and the poor biocompatibility associated with some of them [21, 24, 49]. Strategies for developing and evaluating biomaterials based on both natural and synthetic polymers are central for the advancement of the biomedical field.

Hydrogels composed of thermoresponsive PNIPAM and naturally derived hydrophilic polymers such as chitosan and HA are being studied. In this work, PNIPAM is modified with naturally derived chitosan and HA via EDC/NHS zero-length cross-linking according to a recently reported reaction method with slight modifications [24, 25, 50]. A brief introductory background on PNIPAM, chitosan, and HA general properties is presented here, while published results on their biocompatibility are summarized in the last section of this chapter.

2.2.1. PNIPAM

P(N-isopropylacrylamide) (PNIPAM) is a synthetic, temperature-sensitive polymer that exhibits LCST close to physiological temperature (in the range of 25-32 °C) [21, 46]. Below LCST, hydrogen bonding between the isopropyl side groups of PNIPAM and water molecules dominate and lead to the dissociation of the polymer. The hydrogen bonds become weaker at increased temperatures, while the hydrophobic interactions among polymer hydrophobic segments

become strengthened and dominate, resulting in phase transition (sol-gel) [15, 21, 22, 51].

PNIPAM is polymerized via free radical polymerization. The common initiators used are 2,2'-azoisobutyronitrile (AIBN) and ammonium persulfate (APS) [22, 51-53]. Transfer agents not only control the molecular weight of PNIPAM, but may also be selected to provide reactive end groups (e.g. carboxylic acid or amines) [25, 53, 54]. The LCST of PNIPAM is dependent on MW and co-monomer composition and type. PNIPAM of higher MW exhibits lower LCST compared to shorter PNIPAM chains, because of the higher hydrophobic to hydrophilic segments, especially when the end group is polar [12, 46]. Similarly, incorporating hydrophilic co-monomers increases LCST due to increased hydration in a composition dependent behaviour [55].

Han and Bae observed three temperature dependent transition phases for higher MW PNIPAM and P(NIPAM-co-acrylic acid) that were polymerized in benzene [20]. Upon heating, the polymer precipitated, at cloud point (CP) or LCST, from the aqueous solution but the solution was still a free-flowing solution. In fact, they observed a small reduction in solution viscosity. Longer PNIPAM chains or chains with lower acrylic acid content precipitated first, while the lower MW PNIPAM chains and chains with higher acrylic acid segments remained in random coil conformation. Increasing the temperature resulted in further aggregation of collapsed globules via entanglement with lower MW chains or chains with higher content of acrylic acid. This is defined as the non-flowing gel

phase, whereby the viscosity is increased significantly. The water is expelled and a shrunken gel is formed in the last phase. In addition to the effect of MW and co-monomer content, solution concentration is another critical factor in phase transition behaviour.

Since 1997, very few research publications have addressed the three distinct transition phases well. More specifically, most papers report LCST without reference to gelling temperature or concentration. LCST is the temperature at which the polymer solution becomes opaque. It might not be the same as the gelling temperature. LCST is determined from absorbance measurement at the appropriate temperature range [24, 56]. The critical gelling concentration (CGC), which is the concentration at which PNIPAM or PNIPAM-based polymers gel, can be determined by various means of which inverted-tube is the most common [21].

PNIPAM microgels are more extensively studied compared to linear or crosslinked PNIPAM polymers. However, some research has been recently directed towards modifying the biological, mechanical, and physical properties of PNIPAM while maintaining LCST below 37 °C. For example, chitosan, PEG, and hyaluronic acid have been conjugated to PNIPAM to improve its mechanical properties and biocompatibility [23, 24, 57]. The LCST of linear PNIPAM-COOH in the molecular weight range of $1.3x10^3$ to $2.1x10^4$ Da is in the range of 27.8-30.3 °C, with the longer chains exhibiting lower LCST [25, 53]. Grafting chitosan to PNIPAM did not influence the LCST, but solution viscosity was increased

above LCST [25]. In contrast, grafting HA to PNIPAM (HA-g-PNIPAM) resulted in an increase of LCST to 32 °C for PNIPAM of $6.1x10^3$ molecular weight and 22.1-49.2% HA graft ratio, and to 30 °C for PNIPAM of $1.12x10^4$ molecular weight and 47-72% HA graft ratio [58]. The LCST for PNIPAM alone was not reported in either of the two articles, but relating the size of PNIPAM used to the LCST determined in other articles indicate that LCST was increased. The viscosity of the solution was decreased with higher HA graft ratio [54, 58].

In situ forming hydrogels offer various advantages in biomedical applications such as providing a means of non-invasive and controlled cell and drug delivery. The potential of PNIPAM in drug delivery devices has been investigated for a while, whereas its potential in tissue engineering has not yet matured. Injectable PNIPAM hydrogels are being investigated in soft tissue augmentation, in articular cartilage regeneration, and ocular applications [6, 49].

2.2.2. Chitosan

Chitosan is a natural polysaccharide obtained by deacetylation of chitin, which is obtained from shells of crab, shrimp, lobster, and krill. Chitosan is hydrophilic, biodegradable, and of low toxicity. Chitosan is mainly degraded enzymatically via lysozyme [5, 19]. The polyelectrolyte nature of chitosan is responsible for its mucoadhesive and free-radical scavenging properties. Furthermore, the polyelectrolyte nature of chitosan enables the formation of

temperature-responsive polymers by grafting the appropriate amount of PEG [15].

Chitosan is available in various molecular weights and degrees of deacetylation, both of which are important to its *in vivo* fate. Blood compatibility and cell viability after parenteral application have been shown to depend on chitosan molecular weight and degree of deacetylation. The degradation rate decreases with an increase in the degree of deacetylation [5, 59].

Chitosan is not soluble in water at pH>6, but is soluble in water and forms viscous solutions at lower pH. Different methods of obtaining low-molecular weight and water soluble chitosan have been described [60]. Moreover, chitosan could be coupled to other polymers through the hydroxyl and/or amide groups. Chitosan and chitosan derivatives are employed in a wide range of drug delivery, gene therapy, and tissue engineering applications [61].

2.2.3. Hyaluronic Acid

Hyaluronic acid (HA) is the most extensively studied hydrogel due to its biocompatibility, unique viscoelastic properties, high permeability, high water content, and physical properties [16]. In addition to controlled drug delivery systems, HA has shown a potential in various tissue engineering applications, such as soft tissue augmentation, articular cartilage regeneration, artificial skin, facial intradermal implants, and wound healing [14, 16].

HA is a naturally occurring polysaccharide composed of alternating N-acetyl–β-D-glucosamime and β-D-glucuronic acid units. The highest content of HA is found in synovial fluid, in umbilical cords, and in the vitreous humor of the eye [16]. HA is a major constituent of the extracellular matrix (ECM) serving mechanical, rheological (e.g. act as lubricant and shock absorbent), and biological functions [5, 14, 16]. HA regulates cell behaviour during embryonic development, healing processes, and tumor development [62, 63].

Three groups of HA-specific receptors that mediate interactions with HA have been identified on various cells including epithelial cells, leukocytes, fibroblast, and chondrocytes: CD44; receptor for HA-mediated motility (RHAMM); and intracellular adhesion molecule-1 (ICAM-1). These receptors are responsible for mediating various physiological events, such as cell aggregation, migration, proliferation, and activation [64-66].

The role of HA in promoting and mediating wound healing is highlighted by its abundance in every stage of wound healing [67, 68]. It has been observed that HA induces inflammation and enhances cellular infiltration in a dose-dependent manner. Furthermore, CD44, RHAMM, and ICAM-1 facilitate the migration of cells for the formation of granulation tissue. Contradictory to its initial stage of promoting inflammation, HA plays an important role in moderating inflammation though protecting against free-radical cells [69].

In addition to its physical and chemical properties, the ability of HA to mediate healing processes is of interest in biomaterial applications. The

implantation of biomaterials is always associated with tissue injury that initiates wound healing processes. Unlike normal healing, biomaterials induce foreign body healing that results in the formation of a 50-200 μm thick fibrous capsule. Fibrous capsules impede the performance of biomaterials. It is important to realize that the goal is to induce normal healing processes rather than to inhibit healing through complete hindering of cell interactions with biomaterials [1, 7, 40]. Engineering HA based biomaterials to direct normal wound healing holds great promise for various biomaterials applications.

Some of the literature has considered HA as a non-fouling surface in spite of the increasing number of reports on the ability of HA to support chondrocyte attachment and growth [24, 63]. This counter-effect on protein and cell adhesion is explained by the effect of crosslinking [16, 18]. Additionally, uncrosslinked HA has a very short half life of 0.5-2.5d in tissues [5]. There are two mechanisms of HA degradation: slow degradation via hyaluronidase; and, fast degradation via hydroxyl radicals [5]. Studies have demonstrated that both cell adhesion as well as the rate of degradation are dependent upon the extent of HA crosslinking. The degree of crosslinking is reflected in the relative amount of carboxyl and hydroxyl groups that are converted to ester bonds, which could be indirectly measured by contact angle method [16].

Crosslinked HA is a hydrogel, with high water retention ability and a porous microstructure. Crosslinking HA with low molecular-weight crosslinkers like glutaraldehyde [70], carbodiimide [71], disulfides [17], and polyvalent

hydrazides [72], results in a highly swollen permeable network. The high toxicity of most crosslinking agents led scientists to develop photochemical and thermal means of crosslinking [73].

As an alternative to crosslinking, coupling reactions are being employed to improve the chemical, physical, and mechanical properties of HA. Examples of such reactions include sulfation, esterfication , and etherification to add functional groups [18, 74].

Photopolymerization of glycidyl methacrylate-HA (GMHA) conjugates were synthesized with 5, 7, and 11% methacrylation content [75]. GMHA hydrogels with 11% methacrylation showed a 10 fold decrease in the rate of degradation compared to GMHA hydrogel with 5% methacrylation *in vitro* at low hyaluronidase concentration. Similarly, disulfide-crosslinked hyaluronan (HA-DTPH) and oxidized thiolated HA (HA-DTPH-O) has been shown to decrease the rate of degradation *in vitro* and *in vivo* [17]. The literature on controlling HA degradation is enormous but not much has been published on the host response to HA and HA derivatives.

2.3. Biomaterials and Immunity

The immune system, from a biomaterials point of view, is a double-edged sword. While the immune system merits appreciation for its powerful ability in protecting organisms against infectious agents, it is an obstacle to the success of

biomaterials in various applications (with the exception of vaccine adjuvants). Immune rejection remains the greatest challenge to biomaterial applications, especially when the biomaterial is intended for relatively long use such as in tissue engineering, gene therapy, and controlled release applications.

Regardless of their application, foreign substances are always recognized as a threat by the immune system [11]. The immune system recognizes any biomaterial as foreign and triggers a strong defence mechanism that results in either clearing or isolating the biomaterial with fibrous tissue.

The first part of this section introduces the immune system along with its powerful and highly organized defence mechanism against infectious agents. The second part focuses on immune response to biomaterials and highlights the most recent findings in this area.

The immune system is a group of specialized cells and various types of proteins specialized in protecting organisms against infectious agents. Immune response to infectious agents is triggered by the immune system's ability to recognize infection agents and consequently activate itself to destroy it. The immune system is empowered with innate defence mechanisms (innate immunity) that provide the first line of defence, and a stronger and more specialized form of defence known as adaptive immunity. By convention, the terms immune response and immune system refer to adaptive immunity unless stated otherwise [76].

2.3.1. Innate Immunity

Physical and chemical barriers, blood proteins, phagocytes, natural killer cells, and cytokines are what compromise the innate immune system. Plasma proteins, such as proteins of the complement system, mannose-binding lectin (MBL), and C-reactive proteins are the microbial recognition components of the innate immune system. These proteins recognize the characteristic structures of microbial pathogens through different pathways and present them to phagocytes[7, 76]

2.3.2. Complement System

The complement system is able to recognize microbes through three different pathways: classical; alternative; and lectin. The classical pathway is triggered by the detection of plasma proteins called C1, IgM, IgG1, or IgG3, bound to microbial surfaces. The activation of the alternative pathway is through direct recognition of microbial substances. The lectin pathway is triggered by the recognition of MBL bound to microbial surfaces [7, 76-78].

Complement recognition of microbial substances by any pathway initiates activation of the complement system and results in recruitment and assembly of additional complement proteins into a protease complex. Complement component 3 (C3) cleaves into C3a and C3b. C3a chemoattracts neutrophils and

stimulates inflammation, while C3b covalently bounds to microbial surfaces and serves as an opsonin to promote phagocytosis of microbes [78].

2.3.3. Phagocytes and Natural Killer Cells

The innate system is empowered by the ability of macrophages and neutrophils (phagocytes) to identify, ingest, and destroy microbial substances and to migrate to the site of infection within a few hours of microbial entry. Neutrophils migrate faster to the site of infection, but macrophages persist much longer due to their longer lifespan. Unlike neutrophils, macrophages can undergo cell division at the infection site. Moreover, activated macrophages play an important role not only in innate immunity but also in the effector phase of adaptive immunity [7, 76].

Upon activation, phagocytes secrete regulatory proteins called cytokines. Cytokines are the communication signals between immune cells and between immune cells and respective tissue cells, such as vascular endothelial cells. For example, IL-1, IL-4, TNF-α, and chemokines are known as inflammatory cytokines. These cytokines provide a signal for the activation of phagocytes and recruitment to the site of infection. IL-10 and IL-13 are examples of anti-inflammatory cytokines. IL-6 provides a signal for the activation of adaptive immunity [7, 76].

The innate immune responses not only stimulate the adaptive immune

system, but also influence the nature of defence. On the other hand, and as will be shown later, adaptive immune responses often enhance the antimicrobial activities of defence mechanisms of innate immunity [7, 76].

2.4. Adaptive Immunity

The main components of the adaptive immune system are lymphocytes and antibodies. However, aside from activated lymphocytes, activated innate cells are the main role players in the effector mechanisms of the adaptive immune response. Lymphocytes include B-lymphocytes (B-cells), and two types of T-lymphocytes (helper T-cells and cytotoxic T-cells). Adaptive immune responses are of two types: (i) humoral; and, (ii) cellular. Humoral immunity is the main defence mechanism against extracellular microbes and toxins, while cellular immunity reacts against intracellular microbes that survive and proliferate inside phagoyctes and other host cells [7, 76, 79].

Humoral immunity is mediated by antibodies produced by B-cells. Antibodies have various functions such as microbial recognition, neutralizing infectivity of microbes, targeting microbes for elimination, and activating different effector mechanisms. Cellular immunity is mediated by the two types of T-cells. Helper T-cells produce cytokines (to activate macrophages and B-lymphocytes), while cytotoxic T-cells kill infected cells. Specificity, diversity, memory, specialization, self-limitation, and non-reactivity to self are special features of

adaptive immunity [7, 8, 76, 79, 80].

Immune responses occur in four distinct phases: antigen recognition; the activation of lymphocytes; the effector phase of antigen elimination; and finally, the return to homeostasis and the maintenance of memory.

2.4.1. Antigen Recognition

Antigens are recognized by B-cells via membrane-bound or free antibodies and by T-cells via T cell receptors (TCR). Antibodies are only produced by B lymphocytes, but activated T cells can also participate in humoral immune responses through activating B cells to produce antibodies. Antibodies recognize almost every kind of biological molecules. Sugars, lipids, metabolites, autacoids, hormones and macromolecules such as complex carbohydrates, phospholipids, nucleic acids and proteins are examples of antigen recognizable molecules. However, only macromolecules are able to stimulate B cells to produce antibodies and initiate humoral immune responses [76, 81]. An agent that is capable of inducing immune responses is termed immunogen. Antibodies bind only to a portion of a large antigen, such as macromolecules, termed the epitope.

Antibodies are present in biological fluids though out the body (e.g. in plasma, mucosal secretions, and in the interstitial fluids of the tissues) [76, 81]. Antibodies interaction with antigen is mediated by various types of noncovalent, reversible binding forces, such as electrostatic forces, hydrogen bonds, van der

Waals forces, and hydrophobic interactions. TCR antigen recognition is different from antibody recognition in two ways. First, antibodies can recognize a wide range of molecular classes while TCR can only recognize peptide. Second, while antibodies can recognize bound and free antigens, TCR only recognize peptides processed and presented by other cells [76, 81].

Antigen-presenting cells process the peptide based antigen by displaying it with specialized proteins called the major histocompatibility complex (MHC). T cells have specific ligands that recognize complexes of foreign peptide and self MHC. There are three classes of MHC molecules. Class I and II are membrane-bound glycoproteins, whereas class III encodes genes that participate in immune functions, such as the complement system. Class I molecules are presented by APCs infected with the peptide. Class I molecules induce CD8+ cytolytic T lymphocytes activation to kill infected cells. Class II molecules present peptides to CD4+ helper T cells, which in turn release cytokines that activate B cells and macrophages [76, 81, 82].

2.4.2. Lymphocyte Activation

The recognition of peptide-MHC complexes on APC surfaces by T cells induces their activation and mediates subsequent events though secretion of cytokines and direct interaction with other cells. In addition to secreted cytokines and recognition of peptide-MHC complexes, accessory molecules, such as

costimulators are important in T cell activation. The main cytokine produced by activated T lymphocytes is interleukin 2 (IL-2), which functions as a growth factor for T cells. Hence IL-2 production leads to T cell proliferation through an autocrine activation pathway. T cell activation results in increased expression of receptors for many cytokines. The expression of leukocytes adhesion molecules (L-selectin) decreases, whereas the expression of ligands for E- and P-selectins and CD44 increases. As a result, activated lymphocytes are able to migrate to any site [76, 81-83].

Activated T cells may differentiate into effector or memory cells. Examples of such are T_H1 and T_H2 effector CD4+ helper T cells, which act to activate macrophages and B lymphocytes in the effector phase of cell-mediated and humoral immunity. The effector CD8+ subsets, CD8+ cytolytic T lymphocytes, kill infected cells expressing the class I MHC-antigen complex. Like naïve T cells, memory cells circulate through lymph nodes until encountering an antigen, but memory cells responses are faster and stronger to the specific previously encountered antigens [76, 81-83].

B cells are activated via antigen binding to membrane IgM or IgD receptors or through CD4+ helper T lymphocytes induced activation. B cells activation mediates humoral immunity though secretion of antibodies. Additionally, activated B cells can undergo differentiation to memory and effector B cells. Humoral immune responses are triggered in the peripheral lymphoid organs but secreted antibodies are distributed though out the body to perform

their protective function. As is the case with memory T cells, secondary B cell responses are faster and stronger compared to primary responses [76, 81-83].

2.4.3. Effector Phase

Activated lymphocytes eliminate the antigen in the effector phase of adaptive immune response. Extracellular antigens are eliminated by antibodies, whereas intracellular antigens are eliminated by T lymphocytes. The former involves humoral immune mechanisms while the latter involves cell mediated immune mechanisms. Some components of the innate immune system, such as macrophages and neutrophils, participate in the effector phase, but their phagocytosis capability is greatly enhanced by the adaptive system. Hence the adaptive immune response provides enhancement to the mechanisms of innate immunity [76, 81-83].

2.4.3.1. Cell-mediated Immunity

In cell-mediated immunity, activated T cells eliminate antigens bound to antigen-presenting cells through activating macrophages to produce potent microbicidal agents that kill phagocytosed microbes or through inducing infected cells to undergo apoptosis. Macrophages are activated through the secretion of IFN-γ and other cytokines by effector T_H1 and $CD8^+$ T cells. IFN-γ secretion

induces macrophages to express high levels of surface protein (CD40), for which activated $CD4^+$ T_H1 and $CD8^+$ T cells have a specific ligand. This intracellular signal transduction pathway leads to activating macrophages to carry the effector function of cell-mediated immunity [76, 81-83].

The effector functions of activated macrophages include killing phagocytosed microbes though producing potent microbicidal reactive oxygen intermediates, nitric oxide, and lysosomal enzymes. In addition, activated macrophages play an important role in mediating acute inflammation through secreting various cytokines, such as TNF-α and IL-1, chemokines, and short-lived lipid mediators. Acute inflammation is characterized by local accumulation of neutrophils. Finally, activated macrophages mediate tissue repair through secreting growth factors that stimulate fibroblast proliferation, collagen synthesis, and new blood vessel formation or angiogenesis [76, 81-83].

The progressive secretion of cytokines and growth factors by macrophages that fail to eliminate the infection results in tissue injury followed by formation of connective tissue (fibrosis) at the site of infection. Fibrosis is a hallmark of chronic delayed-type hypersensitivity (DTH) reactions. The persistent cytokine secretion alters the morphology of macrophages. They develop increased cytoplasm and cytoplasmic organelles. Moreover, these macrophages may fuse to from multinucleated giant cells [76, 81-83].

Cytolytic T lymphocytes (CTLs) bind to antigen-presenting cells (APCs) expressing peptide antigen complexed with class I MHC molecules via antigen

receptors and accessory molecules, such as CD8 and LFA-1 integrin. The recognition of CTLs to MHC-associated peptides induces clustering of T cell receptors to generate biochemical signals that lead to the activation of CTLs. Upon activation, the cytoskeleton of CTLs is rearranged in order to move the microtubule organizing center of the CTLs to the area of the cytoplasm near the contact with the infected cells. With this rearrangement, CTLs are able to deliver cytotoxic granule proteins that trigger apoptosis of the target cells [76, 81-83].

2.4.3.2. Humoral Immunity

Humoral immunity is mediated by B lymphocytes through the production of antibodies. Antibodies' effector functions include antigen neutralization, activation of the complement system, and elimination of microbes through enhanced phagocytosis by antigen opsonisation and antibody-dependent cell mediated cytotoxicity. Humoral immunity is systemic, although the activation of B cells occurs in lymphoid tissues because secreted antibodies are distributed throughout the body. Antibodies that mediate humoral immunity may be produced by long-lived antibody-producing plasma cells or activated memory B cells [76, 81-83].

Microbes invade host cells through binding to cell surface molecules. Antibodies neutralize microbes through blocking their binding sites. The affinity of antibodies to microbial binding cites determines their ability in neutralizing

invading microbes. Only the antigen-binding site of an antibody is required for the neutralization of microbes. Most antibodies that lie within this class are of IgG isotype, which are abundant in the blood [76, 81-83].

Some antibodies are able to markedly enhance the phagocytosis ability of macrophages and neutrophils through opsonization. Opsonization is the process by which an antibody (IgG isotype) coats microbes and mediates binding to Fc receptors on phagocytes, thereby promoting phagocytosis. In addition to IgG, microbes may be opsonised by products of the complement system (e.g. C3b). These processes provide another mechanism by which adaptive immunity enhances innate immune responses. In addition, antibody-mediated NK cells and leukocytes binding through Fc receptros results in the killing of these cells in a process termed antibody-dependent cell-mediated cytotoxicity [76, 81-83].

2.5. Inflammation and Wound Healing

The immune system is empowered with powerful wound healing processes. Wound healing is initiated by cell or tissue injury through the release of intracellular components that activate macrophages [7]. Activated macrophages direct wound healing by first cleaning the wound site and then secreting the appropriate cytokines [40]. The normal wound healing mechanism starts with inflammation, which is the infiltration of leukocytes, followed by the formation of vascular granulation tissue. Inflammation is of two phases: the initial

phase is characterized by the infiltration of leukocytes dominated by neutrophils (acute inflammation); while macrophages dominate leukocytes in the second stage (chronic inflammation) [7, 10, 11, 68]. The extent of injury determines the severity of inflammation and duration of each of its stages [7]. Neutrophils and lymphocytes play an important role in wound healing mechanisms, but macrophages prove to be the orchestrators of every stage of wound healing.

The detailed mechanism of inflammation is presented here. IL-1 and TNF secreted by macrophages at the site of the injury trigger endothelial cells of adjacent postcapillary venules to express several adhesion molecules, such as E-selectin [7, 76]. The low binding affinity between ligands (expressed on circulating leukocytes) and selectins results in leukocytes rolling until the arrival of chemokines from the infection site. Chemokines activate rolling leukocytes through conversion of integrins to a high affinity state that supports the firm binding of leukocytes to the vascular endothelium. Chemokines then act on the adherent cells and stimulate the cells to migrate through interendothelial spaces towards the infection site. The consequence of this process is the rapid accumulation of circulating macrophages and neutrophils at the site of the microbial infection [7, 8, 10, 76].

In brief, activated phagocytes produce stimuli for the activation of circulating phagocytes, which ultimately leads to the recruitment of circulating phagocytes to the site of infection.

2.6. Biomaterial-Induced Immune Responses

Organ failure caused by cancer, kidney failure, accidents, unhealthy lifestyles, genetic deficiencies, aging, and other factors, is a leading cause of mortality [84]. In cases where surgical reconstruction is not possible, transplantation becomes the only alternative. The high demand for donated tissues is met only in very low percentages and is often challenged by immune rejection [85]. Although the immune system lacks a specific response mechanism against non-biological material, non-specific responses should not be underestimated [7, 10]. To varying extents, the interaction of biomaterials with the biological system has always led to the activation of a cascade of non-specific immune reactions [7, 8, 10, 11].

Blood-contacting materials, such as stent and cardiovascular devices, trigger reactions different from materials or devices that do not come in direct contact with blood. The former type of interaction results in thromboembolic complications, while the latter results in foreign body reaction (FBR) [7]. Both types of non-specific responses are initiated by the rapid (within seconds post implantation) adsorption of proteins to the surface of the biomaterial. However, the subsequent cascade of events differs between the two types of non-specific responses. Blood-contacting materials are mediated by activated platelets, while FBR is mediated by leukocytes [86]. Acute inflammation, chronic inflammation, foreign body reactions, granulation tissue formation and fibrosis constitute the

common phases of immune response to non-blood-contacting biomaterials.

2.6.1. Proteins

Protein adsorption to biomaterials could be considered the recognition phase. The adsorption of proteins to the surface of a biomaterial depends on protein affinity to the surface, concentration of proteins, and the kinetics of adsorption and desorption. Proteins could be classified as inflammatory, such as complement proteins, fibrinogen, and antibodies (IgG), passive, and adhesion proteins. Adhesion proteins encompass inflammatory proteins that mediate the activation of leukocytes and adhesion to biomaterial surfaces, in addition to proteins that aid in the adhesion and spreading of non-inflammatory cells [7, 8, 10, 11].

Neutrophils and macrophages express receptor proteins for the opsonization of inflammatory proteins, including antibodies. These receptors play a major role in the activation of the attached neutrophils or macrophages. Activated neutrophils and macrophages secrete different types of mediator proteins and cytokines to recruit more leukocytes and mediate inflammatory reactions [7, 8, 10, 11].

2.6.2. Acute and Chronic Inflammation

The placement of a biomaterial *in vivo* always entails tissue injury through injection, insertion, or surgical implantation. Tissue injury initiates inflammatory responses correlated in magnitude to the extent of injury. Tissue injury also accompanies changes in vascular flow, caliber, and permeability of adjacent blood vessels. These changes assist in the exudation (escape from vascular stem into infected or injured tissue) of cytokines followed by leukocytes cells. It is important to note that while inflammation is initiated by leukocytes, it is mediated by cytokines produced by activated cells. Cytokines and the release of other biochemicals are in turn dependent upon the features of the biomaterials, such as size, shape, and chemical and physical properties [7, 8, 11, 30].

Inflammatory reactions are noted in two stages: acute; and, chronic. Acute inflammation is mediated primarily by neutrophils and to a less extent by macrophages. As a result, acute inflammation is of relatively short duration. The major role of neutrophils in acute inflammation is to phagocytose foreign materials through engulfment and degradation. The size of biomaterials hinders such intention and brings neutrophils to frustration. "Frustrated phagocytosis" causes the extracellular release of leukocyte products in an attempt to degrade the biomaterials [7].

Extended release of chemoattractants brings acute inflammation to an end. In most cases, acute inflammation is replaced by chronic inflammation.

Chronic inflammation is characterized by the presence of monocytes, macrophages, and lymphocytes with proliferation of blood vessels and connective tissue. Through communication with lymphocytes, macrophages play the most important role in chronic inflammation. Table 2-2 lists the important classes of products produced and secreted by macrophages [87].

Table 2-2: Products secreted by activated macrophages.

Groups of Substances	Example of products
Reactive oxygen intermediates	Superoxide, hydrogen peroxide, hydroxyl radical, chloramines [88]
Reactive nitrogen intermediates	Nitric oxide, nitrites, nitrates [89]
Tissue damaging	IL-1, TNF-α, IL-6 ref
Complement components	C1, C2, C3, C4, C5, factors B, D, P, I , H ref
Clotting factors	V, VII, IX, X, prothrombin, plasminogen activator, plasminogen activator inhibitors
Cytokines	IL-1, IL-6, IL-8, TNF-α, INF-g, MIP-1, MIP-2, and MIP-3, regulatory growth factors (M-CSF, GM-CSF, G-CSF, PDGF)
Immune response regulators	Macrophage migration inhibitory (MIF), IL-12, IL-18
Tissue regeneration	Elastase, collagenase, hyaluronidase, bFGF, TGF-α, GM-CSF, M-CSF, vascular endothelial growth factor/vascular permeability factor (VEGF/VPF), IL-8, human angionenic factor (HAF) ref

In an attempt to phagocytose the foreign material, monocytes and macrophages fuse to form foreign-body giant cells (FBGCs). The inability of macrophages to engulf or degrade the relatively large biomaterial leads to the release of enzymes, cytokines, and chemical mediators that cause harm to the extracellular environment and, ultimately, damage to adjacent tissues [7, 8].

Extended inflammation (weeks of acute or months of chronic inflammation) is a sign of an infection. The extent of each type of inflammation and overall inflammation is dependent upon the type of biomaterial.

2.6.3. Granulation Tissue

The proliferation of vascular endothelial cells and fibroblast at the implant site forms the hallmark of healing inflammation – granulation tissue. Endothelial cells proliferate, mature, and form new capillary vessels in a process known as angiogensis or neovascularization. Fibroblasts, on the other hand, synthesize proteoglycan (in early stages of granulation) and then collagen, especially type III collagen. Proteoglycan and collagen together constitute the fibrous capsule [7].

2.6.4. Foreign Body Reaction

Foreign body reaction (FBR) is characterized by the presence of granulation tissue and FBGCs and may persist for the lifetime of the implant.

Despite isolation of the implant by fibrosis tissue, it is not known whether large FBGCs remain activated or become quiescent [7, 8].

2.7. Where Are We Now?

Despite the great efforts that have been directed towards developing biomaterials, there are yet not many biomaterials that can truly be termed biomaterials. The first criteria for biomaterials, biocompatibility, has not been met except for limited applications (e.g. contact lenses), because of our incomplete understanding of the mechanisms of host cell interactions with foreign materials [40, 44, 45]. It has been accepted that the adsorption of a non-specific monolayer of proteins to the surface of a material immediately following implantation impairs normal healing and mediates foreign body reactions. The first measure for biocompatibility has, therefore, been correlated with inhibition of non-specific protein adsorption [3].

While many groups have reported the development of materials that inhibit or reduce non-specific protein adsorption and monocyte/macrophage activation *in vitro*, most of the *in vivo* findings did not correlate with *in vitro* results [1, 3, 7]. Bridges *et al.* suggested that a possible explanation for the inconsistency between *in vitro* and *in vivo* results may be the insufficient non-fouling behaviour, coating degradation, and inflammatory mechanisms independent from protein adsorption [90]. Although these are important factors, we must agree that most *in*

vitro systems employed do not fully mimic the *in vivo* complexity of the immune system. This becomes clear when noting the contributions of James Anderson's group, over the past 30 years, in developing an *in vitro* method that closely mimics the *in vivo* complexity of the immune system [10, 11, 30, 91-105].

It is fair to say that James Anderson has contributed significantly to the understanding of the interaction between blood and biomaterials. In 1995, Anderson's group discovered the cytokine, IL-4, that is responsible for inducing the fusion of macrophages to form foreign body giant cells (FBGCs) [94]. This observation is very important in advancing cell culturing techniques and in understanding foreign body reactions. In 2005, Anderson's group presented a more accurate *in vitro* method for the evaluation of biomaterials-induced host responses [100]. The group presented a co-culture system of lymphocytes and monocytes/macrophages and demonstrated the role lymphocytes play in mediating host reaction through interaction with macrophages. They showed that co-culture systems induced higher level of monocyte adhesion and fusion [35, 100, 103]. Despite this important finding, *in vitro* assays on biomaterials-induced inflammation have often included monocyte/macrophage only in cell culture systems [106-108].

In addition, the relationship between cell adhesion and activation was redefined by Anderson's group in 2007 [109]. Prior to that, inflammatory cell adhesion was correlated with cell activation [3, 30]. Although cell adhesion was directed by surface chemistry, such that hydrophilic neutral and negatively

charged hydrophilic surfaces induced lower levels of monocyte/macrophage adhesion, proteomic analysis revealed an inverse relationship of cell adhesion and activation. Cells adherent to hydrophilic surfaces increased the release of cytokine 2-83 fold compared to cells on hydrophobic surfaces. The selected cytokines were IL-1β, IL-6, IL-8, MIP-1β, and IL-10. Thus, cells can be activated to varying degrees and produce varying responses. The group suggested that a phenotypic switch in macrophage phenotype from classically activated to alternatively activated occurred early during the course of culture (day 3). This phenotype switch was independent of surface chemistry. It is needless to mention that the vast majority of *in vitro* studies do not include various time points let alone consideration of cell phenotypic switch.

In vivo biocompatibility measures have been related to the divergence from normal wound healing and extent of fibrous capsule formation. The duration and severity of acute inflammation and chronic inflammation determines the fate of the materials [1, 40]. Depending on its thickness, a fibrous capsule could impair a biomaterials' function through blocking or reducing drug release rate or preventing materials integration with other tissues in the case of tissue engineering applications. Strategies for reducing the extent of host response include introducing micro- or nano- details, incorporation matricellular proteins, and utilizing hydrogels [1, 7, 9, 30, 40, 44, 102, 104]. This section will present the up-to-date biocompatibility studies on hydrogels in general and on PNIPAM, chitosan, and HA based materials.

2.7.1. Host Response to Hydrogels

Hydrogels applications in the biomedical field have expanded over the past ten years. This could explain the limited number of published works on *in vivo* host response to hydrogels. Hydrogels are thought to inhibit or reduce protein adsorption to biomaterials because of their: (i) low interfacial free energy that has no affinity for protein adsorption; (ii) high chain mobility; and, (iii) soft nature [7, 40, 110]. This section illustrates if this assumption is correct. Factors that contribute to the ability of hydrogels to resist protein adsorption are also considered.

The immune response to gelatin-based hydrogel systems was evaluated by Stevens K. R. *et al* utilizing a subcutaneous cage implant system [111]. Gelatin is a hydrophilic protein prepared from the partial hydrolysis of collagen. Gelatin is biodegradable and induces low levels of immunogensicity and cytotoxicity. The group compared immune response to interpenetrating networks of gelatin and poly (ethylene glycol) diacrylate (PEGdA) compared to glutaraldehyde crosslinked gelatin. The percentage of glutaraldehyde fixation, the percentage of PEGdA, and the molecular weight of PEGdA (2-8kD) were varied.

They observed slightly stronger inflammatory response to gelatin-based hydrogel systems compared to the rapid inflammatory response elicited by empty cage controls, but the response was dependent upon the percentage of glutaraldehyde fixation or the percentage of PEGdA. The empty cage controls,

gelatin hydrogels without glutaraldehyde fixation, and gelatin hydrogels with low glutaraldehyde fixation (below 0.01%), elicited a rapid acute inflammatory response that resolved within 4 days and was comparable to chronic inflammatory response (evident from the comparable density of total leukocytes concentration on these surfaces). However, higher concentrations of glutaraldehyde fixation (0.1%) elicited longer acute and chronic inflammation. Similarly, higher percentages of PEGdA (above 40%) induced stronger immune reactions.

The group also studied the effect of incorporating anti-inflammatory dexamethasone into gelatin based hydrogel systems. They observed that the effect was a reduction in leukocyte concentration compared to gelatin hydrogels without dexamethasone. They also observed impaired wound healing and hypersensitive reaction, evident by the absence of the fibrous capsule that was noted with all other samples by day 4.

Non-degradable dextran methacrylated hydrogel (dex-MA) and degradable lactate-hydroxylethyl-derivatized dextran (dex-lactate-HEMA) of varying initial water content and degree of substitution were implanted subcutaneously in rats to evaluate immune response to dextran-based hydrogels [110]. As expected, the study showed that hydrogels with higher water content (90%) produced milder immune response *in vivo*. The study revealed acceptable immune response to dextran-based hydrogels with the rapid resolution of acute inflammation (by day 5) and formation of a fibrous capsule and new blood

vessels. Comparing various degrees of substitution demonstrated that intermediate (DS 9) degree of substitution elicited the least immune response.

The study aimed at comparing immune response to degradable and non-degradable dextran-based hydrogels, but very brief observations were reported. It was reported that degradable dex-lactate-HEMA induced lower initial foreign-body reaction and that degradation was associated with infiltration of macrophages and formation of giant cells. The implanted hydrogel was not present by day 21, but no observations have been reported for the intermediate stage (between 5 and 21 days post implantation). The authors concluded from their reported results that dex-MA hydrogels did not induce an immunogenic response.

A number of published articles on the biocompatibility of biomaterials prove modest understanding of the subject. Examples are presented in a paper published this year on the biocompatibility of polyurethane acrylate (PUA) based hydrogels [112]. Two types of PUAs were surgically implanted and injected in the dorsums of rats with the aim of evaluating the biocompatibility of PUA-based hydrogels compared to poly(methyl methacrylate) (PMMA) over a period of 4 weeks. As noted in Table 2-3 (extracted from the reference), four levels of host response were reported: (i) light inflammation characterized by the presence of lymphocytes; (ii) inflammatory reaction with few giant cells; (iii) fibrous capsule, lymphocytes, and giant cells; and, (iv) encapsulation of the implant. While these are the typical foreign body reactions, the authors claimed that their *in vivo* study

confirmed the absence of tissue reaction to both surgically implanted and injected PUA hydrogels.

Table 2-3: Biocompatibility of PUA based hydrogels. I: light inflammatory reactions. II: evident inflammatory reaction with giant cells. III: fibrosis and presence of lymphocytes and giant cells. IV: foreign body reaction. Reproduced from reference [112].

Implant	Injectable		Surgical	
	2 weeks	4 weeks	2 weeks	4 weeks
PMMA	II	III		
PUA-PPG	II and III	I	II and III	I
PUA-PCL	II and III	I	II and III	I

Surprisingly, the authors did not discuss the prolonged chronic inflammation (2 weeks post implantation) compared to normal healing, fibrous capsule thickness, or formation of new blood vessels. It was noted that PUL-PCL developed a thicker fibrous capsule compared to PUA-PPG implant, but no values were reported and a comparison to PMMA (controls) was not made. Furthermore, the disappearance of fibrous tissue and giant cells was not observed in any of the articles on biomaterials induced responses that I have encountered. Knowing that there are differences between injectable and non-injectable hydrogels in their chemical and physical properties, and knowing that

tissue injury initiates the early stages of immune response and mediates the later stages, it is very unclear how surgically implanted and injectable hydrogels lead to similar reactions. In short, the article presented excellent work in terms of making and characterizing PUA injectable hydrogels, but the biocompatibility study was not convincing.

2.7.2. Host Responses to PNIPAM, Chitosan, and HA

No article has been published on protein adsorption or inflammatory response to linear PNIPAM without modification, mainly because the polymer becomes hydrophobic at body temperature and it is well known that hydrophobic surfaces support high levels of protein adsorption.

Protein adsorption to copolymers of NIPAM and N-tert-butylacrylamide (NtBAAm) prepared with varying NIPAM to NtBAAm content was studied by Allen *L. T. et al* [113]. Increasing the NtBAAm content in the copolymer resulted in slightly increased contact angle due to the increase in $-CH_3$ groups at the expense of the –NH groups of NIPAM. Copolymers were of 50:50, 65:35, and 85:15 NIPAM:NtBAAm ratios. Contact angle ranged from 52.98° to 56.53°, the lowest and highest NtBAAm content, respectively. This slight increase in contact angle associated with NtBAAm incorporation resulted in lower levels of serum protein adsorption and albumin adsorption. However, fibronectin adsorption increased with increasing NtBAAm content. The high NtBAAm content suggested

that the copolymer did not exhibit the LCST of pure PNIPAM. In fact, the article did not mention PNIPAM's thermoresponsive characteristic or the temperature at which protein adsorption was analyzed. The important observation that should be made from this article is that P(NIPAM-co-NtBAAm) of all compositions provided a substrate for protein adsorption.

Bridges A.W. *et al.* evaluated immune response to thin film coating of P(NIPAM-coAA) microparticles cross-linked with poly(ethylene glycol) diacrylate on Poly(ethylene terephthalate) (PET) *in vitro* and *in vivo* [90]. Fibrinogen was selected as the model protein for their protein adsorption study because of its role in mediating the adhesion of platelets and leukocytes. Microgel coating reduced adsorbed protein levels 7 folds compared to unmodified PET surfaces. Adherent cell density, cell viability, and spreading were evaluated after a 48-hour culture of monocytes on PET and microgel-coated PET. Microgel coating reduced monocytes/macrophage adhesion 40 folds compared to unmodified PET. Cells adherent to PET samples had almost twice the cytoplasmic spread area compared to those adherent to the microgel-coated samples. Cell viability was greater than 98 for both surfaces.

The *in vivo* experiments evaluated the adhesion of leukocytes and cytokine release on samples implanted in the intraperitoneal cavity of mice for 48 hours. The results obtained were consistent with *in vitro* results. Compared to PET surfaces, cell density on microgel-coated surfaces was reduced 4.6 fold, and significantly lower levels of pro-inflammatory cytokines (TNF-α, IL-1β, and

MCP-1) were detected.

One year later, the group published their results on chronic inflammatory responses to the same microgel coating [114]. The samples were implanted subcutaneously in rats for 4 weeks, to evaluate fibrous capsule formation. The group observed a 22% thinner capsule layer surrounding microgel-coated surfaces with about 40% fewer associated cells, compared to unmodified PET surfaces. The faster resolution of tissue reaction to microgel-coated surfaces, compared to unmodified PET surfaces, was illustrated by the thinner and more organized structure of the fibrous capsule associated with these surfaces. Interestingly, microgel coating did not utilize the thermoresponsive property of PNIPAM. It is very likely that the results observed were due to: (i) the presence of non-fouling PEG; (ii) the submicron architecture of microgel-coated surfaces; and, (iii) the increase in LCST of PNIPAM, possibly above body temperature, due to the presence of hydrophilic components.

The temperature sensitivity of PNIPAM is far more advantageous in drug and cell delivery and gene therapy applications than in tissue engineering applications due to the limited possible applications where injectable scaffold is feasible. Injectable materials are advantageous in terms of ease of application, localization, and non-invasiveness [21, 112]. However, the hydrophobic switch at body temperature presents challenges associated with host responses. It is therefore important to develop modification strategies to improve injectable or PNIPAM-based materials.

2.7.3. Chitosan

Depending on its molecular weight and degree of deacetylation, chitosan may provide interesting properties for biomaterials applications [5, 115-117]. Its hydrophilicity, biodegradability, antibacterial property, and wound healing activities have attracted a great deal of interest [5, 118]. Non-immunogenicity associated with chitosan has been taken for granted by the vast majority of researchers despite the availability of evidence showing variation in levels of host responses to chitosan polymers of various molecular weights and degrees of deacetylation [117]. Additional interesting features of chitosan are the porous structure, gel forming properties, ease of chemical modification, and high affinity to *in vivo* macromolecules [19, 119].

Immune responses to chitosan-based implants were presented in a recently (2008) published article in Biomaterials [19]. The implants comprised of disks of aggregated chitosan particles of 430-450 nm mean size. The implants were implanted intramuscularly. Surprisingly, neither the molecular weight nor the degree of deacetylation of chitosan used were reported. Stereolight micrographs of implants retrieved after time points of 1 to 12 weeks showed continually increasing layers of connective tissue covering the implant. Histological evaluations on retrieved chitosan implants revealed persistence of acute inflammation one week after implantation. Two weeks post implantation, lymphocytes and FBGCs were present with some necrosis that the authors

chose to neglect because of formation of large extracellular matrix around the particles. Smooth muscle actin was present. Three months post implantation, connective tissue cells and lymphocytes were still present.

Thermosensitive chitosan hydrogel composed of 10% glycerol 2-phosphate disodium salt hydrate (β-GP) was injected subcutaneously in mice [120]. Histological examination after 10, 20, and 30 days showed inflammatory signs and formation of fibrous tissue around hydrogels. The paper considered chiosand-β-GP biocompatible without carefully analyzing immune reactions in detail (e.g. severity of inflammation, fibrous capsule thickness, and formation of new blood vessels).

Another injectable chitosan-based formulation was prepared by modification with phospholipids [121]. The hydrogel was injected subcutaneously and intraperitoneally, and sacrifices were performed 1, 2, 3, and 4 weeks post injection. Histological slides were not included in the article and the results were not discussed relative to time points post injection. The main observation reported was that subcutaneous administration resulted in no signs of inflammation and no fibrous capsule was formed. The authors explained that this unusual absence of any signs of inflammation was due to differences in compositions and formulation, such as the inclusion of egg phosphatidylcholine in the formulation. Intraperitoneal injection of chitosan-phospholipid systems resulted in a 3-5 μm think fibrous capsule formation. Another explanation

provided by the group for the extremely low tissue reactions was the use of highly deacetylated chitosan. Highly deacetylated chitosan (more than 73.3 mol%) degraded slower and resulted in reduced extents of tissue reactions.

A lot of work has been directed towards engineering chitosan-based medical and pharmaceutical devices but not much work has been done towards understanding its biocompatibility [122-124]. It should be emphasized that biomaterials must not inhibit immune responses but direct them to normal healing. It is therefore not clear how the biomaterials would perform the desired function while allowing normal healing with the low to no inflammation observed on the injectable chitosan-based hydrogels discussed above.

2.7.4. HA

The *in vivo* immune response to subcutaneously and peritoneally implanted thiolated HA (HA-DTPH) and to the less rapidly degradable HA-DTPH(H_2O_2) was evaluated over a period of 6 weeks by Liu Y. *et al* [125].

Vascularization was observed on both subcutaneously implanted surfaces by day three, but acute inflammation was slightly more mild on HA-DTPH(H_2O_2) surfaces and resolved quicker compared to HA-DTPH. Additionally, lower levels of chronic inflammatory reactions were observed on HA-DTPH(H_2O_2) as evident by the lower macrophage density present on the surfaces. After 42 days post implantation, only a thin fibrous capsule was present around the implants.

Overall, the inflammatory reactions to the two surfaces were mild not significantly different.

Similarly, granulocyte infiltration began to resolve by day three post intraperitoneal implantation of HA-DTPH and HA-DTPH(H_2O_2). HA-DTPH induced the formation of fibrous tissue approximately double the size of that induced by HA-DTPH(H_2O_2) (56.4 μm compared to 28.9 μm), but both are considered thin when compared to fibrosis induced by other materials. It can therefore be concluded that the article presented an excellent form of modified HA that can potentially serve many biomedical applications.

Glycidyl methacrylate-HA (GMHA) conjugates were prepared by crosslinking HA with photopolymerizable methacrylate [75]. The paper focused on characterizing hydrogel physiological parameters, including swelling ratio, stiffness, and enzymatic degradation, while very briefly analyzing immune response to subcutaneously implanted GMHA hydrogels. The group observed minimal immune responses to GMHA hydrogels.

The promise of utilizing HA in biomedical applications is widely accepted in the field but very few published papers present ideal crosslinking or modification methods that yield the desired biocompatibility. This indicates that, as is the case with PNIPAM, a great deal of research needs to be directed towards modifying and evaluating host responses to these interesting biomaterials.

3. Scope of Project

A great deal of work is directed towards the use of injectable biomaterials for various biomedical applications. The general assumption made by researchers in the area is that injectable biomaterials, and hydrogels in general, resist non-specific protein adsorption and ultimately lead to favored biological interaction. However, very little has been published on the immune responses to hydrogels and injectable biomaterials.

In this work we have established a method for evaluating immune response to injectable biomaterials *in vitro* and in vivo. Our models of injectable materials are chitosan grafted, and chitosan-grafted-HA-grafted PNIPAM. PNIPAM is widely investigated because of its desired LCST; close to body temperature. Furthermore, we have studied reaction conditions for all three model polymers and determined the optimum conditions to improve their performance and biocompatibility.

4. Student Contribution

Except for repeats of ELISA, Western-blotting, and TNBS reactions that were performed by undergraduate summer student, the work presented here was entirely done by the author of this thesis. This includes experimental design, performing experiments, and analyzing of experiments.

5. Article

Synthesis, characterization, and evaluation of host response to P(NIPAM-co-acrylic Acid) based hydrogels

This paper describes the synthesis and characterization of P(NIPAM-co-AA), and the grafting of chitosan and HA to P(NIPAM-co-AA). The evaluation of immune response to P(NIPAM-co-AA) and its derivative is also presented in details.

SYNTHESIS, CHARACTERIZATION, AND EVALUATION OF HOST RESPONSE TO P(NIPAM-CO-ACRYLIC ACID) BASED HYDROGELS

Mariam Al-Haydari, Todd Hoare, and Kim Jones

Department of Chemical Engineering

McMaster University

1280 Main St. W., Hamilton, ON

Abstract

Biomaterials are thought to be the magical solution to improving the quality of life and lengthening lifespans of human beings. In addition to possessing the desired mechanical, physical, and biological functions, biomaterials need to escape undesired immune responses. To date, there is no biomaterial that can completely escape immune responses. However, successes have recently been made in reducing immune responses to biomaterials.

PNIPAM, chitosan (CS), and hyaluronic acid (HA) are examples of polymers that are gaining great interest in the field of biomaterials. The most attractive property of PNIPAM is thermo-responsiveness. Adequate literature has been published on improving the mechanical strength of PNIPAM, but not much has been published on host response to PNIPAM based graft-polymers. CS and HA are generally considered non-toxic and non-immunogenic.

The first part of this project focuses on the synthesis and characterization of HA-grafted-CS-grafted-P(N-co-AA), HA-CS-P(N-co-AA), while the second part examines the effect of grafting on the extent of immune reaction compared to P(N-co-AA) alone.

P(NIPAM-co-acrylic acid), P(N-co-AA), was synthesized to increase carboxylic sites available for CS incorporation. The incorporation of CS into P(N-co-AA), and HA into CS-P(N-co-AA) was confirmed by FT-IR, ^{1}H NMR, TNBS and LCST. The optimum Mn for P(N-co-AA) that could provide sufficient amount

of reactive sites while maintaining LCST below 37 °C was found to be in the range of 2-2.5kDa. Western blotting results demonstrated that incorporating CS into P(N-co-AA) reduces the amount of fibrinogen, fibronectin, and vitronectin adsorbed, and eliminates C3 adsorption. Furthermore, incorporating HA eliminates more inflammatory proteins including fibrinogen and reduces IgG adsorption. CS-P(N-co-AA) elicited lower levels of inflammatory cytokine release compared to P(N-co-AA), but higher than P(N-co-AA)-CS-HA. *In vitro* and *in vivo* results revealed lowest density of leukocytes adhesion to HA-CS-P(N-co-AA) surface compared to the other surfaces. The extent and duration of inflammation was reduced on CS-P(N-co-AA) and HA-CS-P(N-co-AA) hydrogels.

5.1. Introduction

The inability to control protein adsorption to biomaterials surfaces induced researchers to investigate hydrogels. Hydrogels are generally considered non-fouling surfaces due to their hydrophilic nature and ability to retain high water content. Among the most widely studied hydrogels are poly(N-isopropylacrylamide), PNIPAM, and hyaluronic acid (HA).

PNIPAM exhibits a LCST below body temperature, thus PNIPAM is hydrophobic at physiological temperature. However, its LCST is advantageous in terms of providing the biomaterial with *in situ* gelling characteristic. Grafting biocompatible polymers to PNIPAM is necessary in order to improve its biocompatibility.

HA is a naturally occurring polysaccharide composed of alternating N-acetyl-β-D-glucosamime and β-D-glucuronic acid units. HA is a major constituent of the extracellular matrix (ECM) serving mechanical, rheological, and biological functions [5]. Crosslinked HA has attracted a great deal of research due to its biocompatibility, unique viscoelastic properties, high permeability, high water content, and physical properties [16].

A grafted polymer network composed of PNIPAM, HA, and chitosan has a great potential as a drug delivery or gene therapy vehicle as well as in injectable tissue engineering application. Chitosan was used to provide mechanical strength and to provide reactive sites for HA. In this work, we have studied

reaction conditions for the synthesis of HA-grafted-chitosan-grafted-PNIPAM (HA-CS-P(NIPAM-co-AA)). Additionally, the immune response to the three types of PNIPAM surfaces was evaluated *in vitro* and *in vivo*. A co-culture system of lymphocytes and monocytes was employed to evaluate inflammation based on the extent of cytokine release.

5.2. Materials and Methods

5.2.1. Materials

All chemicals were purchased from Sigma-Aldrich unless stated otherwise. N-isopropylacrylamide (NIPAM) was purified by recrystallization from a toluene-hexane mixture. Mercaptoacetic acid (MAA), acrylic acid (AA), 1-ethyl-3(3-dimethylaminopropyl) carbodiimide hydrochloride (EDC), N-hydroxylsuccinimide (NHS), 4-morpholinethane sulfonic acid (MES), trinitrobenzenesulfonic acid (TNBS), and hyaluronic acid sodium (HA, molecular weight ~1.6 x 10^6) were used as received. Chitosan (75-85 degrees of deacetylation) was degraded in an aqueous solution containing hydrochloric acid and 5% (v/v) hydrogen peroxide. Dimethyl 2, 2'-azobisisobutylrate (MAIB, purchased from Wako) was the initiator used for NIPAM polymerization.

5.2.2. Synthesis and Characterization

5.2.2.1. Chitosan Degradation

The depolymerization method utilizing hydrogen peroxide was employed to obtain low molecular weight chitosan [56]. A known amount of chitosan (8 g) was added to a 200 mL mixture of DI-water and hydrochloric acid. In order to dissolve the chitosan completely, the mixture was heated to 70 °C for 2 hours. 10 mL of hydrogen peroxide (30%) was then added and the depolymerization proceeded for an additional 5 hours. The fraction of higher MW chitosan was separated by adjusting the reaction pH to 7, followed by centrifugation. The lower MW chitosan dissolved in supernatant was collected by precipitation in ethanol.

5.2.2.2. P(NIPAM-co-AA)

Prior to polymerization, NIPAM was purified by recrystallization from toluene-hexane mixture. NIPAM (30g) was dissolved in 30 mL of toluene at 50 °C. NIPAM crystallization occurred by adding 20 mL of hexane and rapidly cooling the mixture for 3 hours. NIPAM crystals were filtered and air-dried.

A low ratio (6% molar) of acrylic acid was copolymerized with NIPAM to increase the number of carboxylic acid sites at the copolymer backbone for higher chitosan conjugation. The copolymerization of NIPAM and acrylic acid was carried out by free radical polymerization [25, 53]. Briefly, the amounts of

NIPAM, MAA, AA, and MAIB given in Table 5-1 were dissolved in ethanol and the reaction was carried out at 60 °C under nitrogen atmosphere for 24 hours (Figure 5-1). The copolymer was then precipitated in excess amounts of diethyl ether, followed by dialysis (MWCO 1,000) against water to remove residual monomers and reagents. The purified copolymer was freeze-dried and stored at room temperature.

Table 5-1: P(NIPAM-co-AA) polymerization. * mole % AA obtained from NMR. ** Critical gel concentration.

Sample no.	NIPAM/MAA/MAIB	AA/MAA	* mol % AA	LCST	Mn	**CGC (w/v%)
1	100/10/1	0.5	6	NA	NA	NA
2	150/10/1	1	3	33	2367	NA
3	100/2/1	3	1.7		2033	60
4	100/1.3/1	4.5	1.6	32	2583	20

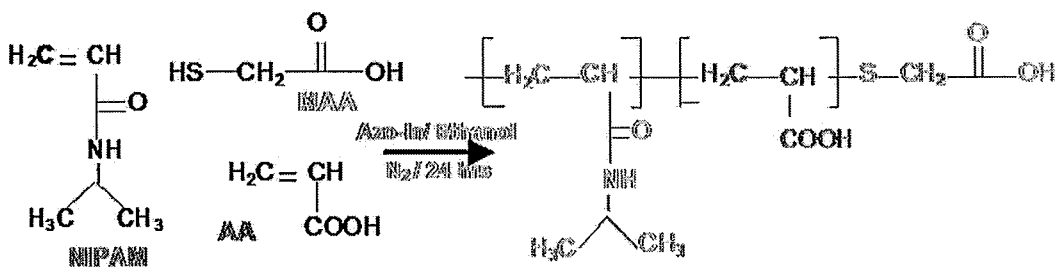

Figure 5-1: Reaction scheme for the polymerization of P(NIPAM-co-AA).

The actual mole fraction of AA to NIPAM on the polymer backbone was determined from ^{1}H NMR spectra. The number average molecular weight of P(NIPAM-co-AA) was determined from AA/PNIPAM fraction and carboxylic acid group titration with 0.1N NaOH.

5.2.2.3. CS-P(NIPAM-co-AA) and HA-CS-P(NIPAM-co-AA)

EDC/NHS zero-length crosslinkers were used to conjugate both chitosan and HA in two separate reactions [24, 25]. First, the carboxylic acid groups of P(NIPAM-co-AA) were conjugated with the amine groups of chitosan in 50 mL of MES buffer (0.1M, 4.5<pH<6) containing 2.2 g of EDC and 0.26 g of NHS. The effect of the EDC/NHS ratio was examined according to Table 5-2. Following 24 hours of reaction, the product was collected by precipitation in sodium chloride. To remove impurities and residual chitosan groups, the product was dissolved in water and precipitation in sodium chloride was carried out an additional two times. The product was then dialyzed against water for 3 days (MWCO 50,000) followed by freeze-drying. Next, the carboxylic acid groups of HA were conjugated with the amine groups of chitosan on the graft polymer using the same procedure above. The product was stored at 4 °C.

The amount of chitosan grafted to P(NIPAM-co-AA), and HA to CS-P(NIPAM-co-AA), were determined by TNBS method. A standard curve was obtained by reacting different concentrations of glycine with TNBS. The

absorbance was read at 335 nm wavelength (Beckman Coulter, DU800 Spectrophotometer).

Table 5-2: The effect of EDC/NHS ratio on chitosan graft yield.

Sample	PNIPAM MW	EDC/NHS (molar)	LCST	CS/PNIPAM (molar)
P-CS1	2033	1/1	35	N/A
P-CS2	2033	1/3	36	N/A
P-CS3	2367	5/1	34	N/A
P-CS4	2367	5/1	N/A	0.004
P-CS5	2367	1/1	N/A	0.152

5.2.2.4. ^{1}H NMR

Freeze-dried samples (50mg) were dissolved in 1 mL D_2O. ^{1}H NMR spectra were acquired using a Bruker AV200 spectrometer operating at 200 MHz.

5.2.2.5. Lower Critical Solution Temperature (LCST)

The effect of copolymerization and grafting CS and HA at phase transition temperature was evaluated using UV/Vis spectrophotometer (Beckman Coulter, DU800 Spectrophotometer). The absorbance of polymer solutions was measured at a wavelength of 470 nm. The temperature was increased for each polymer solution from 25 to 40 °C at 1 °C increments and 5 minutes wait time for

equilibration. The LCST of the polymer solution was defined as the temperature where the solution turbidity is half of the difference between the maximum and minimum values.

5.2.2.6. Critical Gel Concentration (CGC)

A simple test-tube inverting method was employed to obtain samples of CGC. Increments of 20 mg were added to 1 mL of PBS until the gel phase (non-flowing phase) was visually observed. The solutions were incubated at 37 °C for ten minutes with each added mass.

5.2.2.7. Scanning Electron Microscopy (SEM)

Each of the three copolymers was dissolved in miliQ-water at three different concentrations. The samples were incubated at 37 °C for 5 minutes, followed by rapid freezing in liquid nitrogen. Freeze-dried samples were coated with a 5 nm thick platinum layer. A SEM (JEOL, JSM-7000F) was used to visualize the microstructure and pore-size distribution in the polymer gels.

5.2.3. *In Vivo* and *In Vitro*

5.2.3.1. Polymeric Surface Preparation

P(NIPAM-co-AA) and PNA-CS were dissolved in PBS supplemented with 2% antibiotic at a concentration of 0.2 g/mL, while HA-CS-P(NIPAM-co-AA) was dissolved in the same medium at a concentration of 0.1 g/mL. The volume represents the added volume of PBS containing antibiotic. The samples were further sterilized by UV light for at least 30 minutes and were incubated at 37 °C for 24 hours.

5.2.3.2. Western Blotting

Three 2 cm diameter surfaces per sample were incubated with 0.2 mL human plasma at 37 °C. TCPS and glass surfaces were used as controls. After 3 hours, samples were rinsed three times with warm PBS and were incubated with 0.2 mL of 2% SDS solution at 37 °C for a minimum of 12 hours to elute adsorbed proteins. The collected protein solutions were reduced with β-mercaptoethanol at 95 °C for 7 minutes.

SDS page was performed as described elsewhere [126, 127]. Briefly, reduced protein solutions were loaded onto a polyacrylamide gel consisting of 12% (w/v) separating gel and 4% (w/v) stacking gel. The proteins were electrophoresed for 45 minutes at 200 V. The separated proteins on the gel were

then transferred onto a PVDF membrane using the iBlot system (Invitrogen). The blot was cut into strips, blocked with 5% (w/v) solution of nonfat dry milk in 50 mM Tris-buffered saline, and incubated with primary antibody, followed by secondary antibody. Bands were visualized by incubating with NBT/BCIP substrate.

5.2.3.3. *In Vitro* Cell Culture

Human participation was approved by the McMaster University Research Ethics Board (MREB). Human blood monocytes and lymphocytes were obtained from healthy donors and were isolated via a density gradient centrifugation method (Lympholyte-H, Cedarlane), as per the manufacturer's instructions. Isolated cells were cultured in 0.1 mL of macrophage serum-free media containing L-Glutamine (GIBCO) with 20% autologus serum and antibiotic. 50 μL of $7.5x10^6$ cell/mL were seeded on hydrogels and were supplemented with 50 μL of media. At days 1, 5, 7 and 10, supernatants were collected, centrifuged to remove non-adherent cells, and stored at -70 °C for ELISA analysis. Cell viability of the non-adherent cells was assessed using a live/dea kit for mammalian cells (Invitrogen, L3224), as per the manufacturer's protocol. The fluorescence-stained cells were imaged using an inverted fluorescence microscope (Zeiss AxioVert 200).

5.2.3.4. ELISA

Three pro-inflammatory cytokines (TNF-α, IL-4, IL-6) and one anti-inflammatory cytokine (IL-10) were selected to quantify the degree of inflammation caused by PNIPAM based hydrogels. Supernatants were collected from monocytes/lymphocyte cultures at days 1, 5, 7, and 10, and ELISA kits (BioLegend) were used to quantify cytokine release as per the manufacturer's protocol.

5.2.3.5. *In Vivo*

In vivo tests were conducted in accordance with animal utilization protocol (AUP) number 09-06-18 accepted by the Animal Research Ethics Board (AREB) at McMaster University. Female Balb/c mice of 5-7 weeks of age were lightly anesthetized using gaseous anesthesia. The dorsal site of interest was shaved, wiped with alcohol, and injected subcutaneously with 0.2 mL of hydrogels. The mice were kept on a heating pad for ten minutes before recovering to ensure solidification of the implant. At different points in time, the mice were anesthetized using injectable anesthesia (0.2 g/kg Ketamine and 0.01 g/kg Xylazine). Implant sites were cut for histological sampling, and mice were euthanized immediately.

5.2.3.6. Histology

Tissue sections were prepared for histology by fixing in formalin for 48 hours followed by successive dehydrating in increasing concentrations of ethanol. Tissue sections were stained with Hematoxylin and Eosin stain (H & E).

5.3. Results

5.3.1. Synthesis and Characterization

The copolymerization of P(NIPAM-co-AA) was confirmed by ^{1}H NMR, FT-IR, and change in LCST. A typical ^{1}H NMR spectrum with $-CH_3$, backbone $-CH_2$ and –CH, and isopropyl –CH, peaks at 0.975 (peak 1), 1.438 (peak 2), 1.859 (peak 3), and 3.739ppm (peak 5), is shown in Figure 5-2. The peak intensity ratio of peak numbers 1:2:3:5 is 6.1:2.1:1.1:1, which is in satisfactory agreement with the theoretical ratio of 6:2:1:1 [22]. Peak 4 at 3.033 ppm belongs to –CH of acrylic acid. The molar ratio of acrylic acid to NIPAM in the copolymer was determined from peak intensity ratio of 4:5.

The IR spectra are shown in Figure 5-3 and Figure 5-4. IR data of commercial and degraded chitosan were identical. The characteristic absorptions of chitosan are: 3400 cm^{-1} (O-H stretching); 2900 cm^{-1} (C-H stretching); 1660 cm^{-1} (amide I); 1400 (amide II); absorption bands at 1160cm^{-1}, 1083 cm^{-1}, and 1030 cm^{-1} (C-O stretching) were characteristics of its saccharine structure (Figure 5-3)

[22,25,26].

The characteristic peaks of P(NIPAM-co-AA) are: 3342 cm^{-1} (C-H stretching), 1652 and 1538 cm^{-1} (amide bands), and 1360 cm^{-1} (methyl groups). The FT-IR spectrum of CS-P(NIPAM-co-AA) was very similar to that of P(NIPAM-co-AA) but with the presence of broad C-O absorption bands of chitosan at 1082 cm^{-1} (Figure 5-4). The characteristic amide bands of chitosan overlapped with those of P(NIPAM-co-AA).

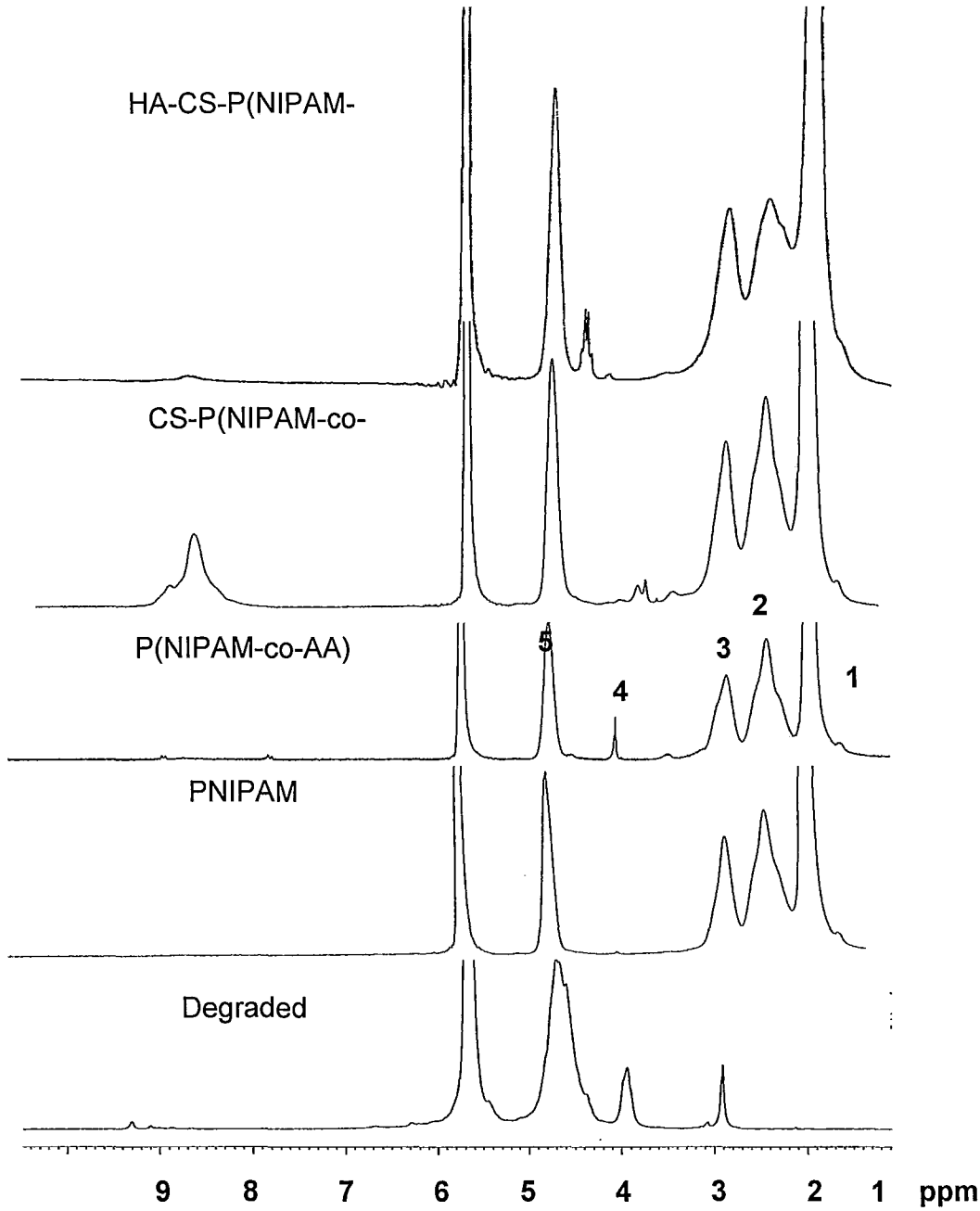

Figure 5-2: 1H NMR Spectra of samples dissolved in D2O.

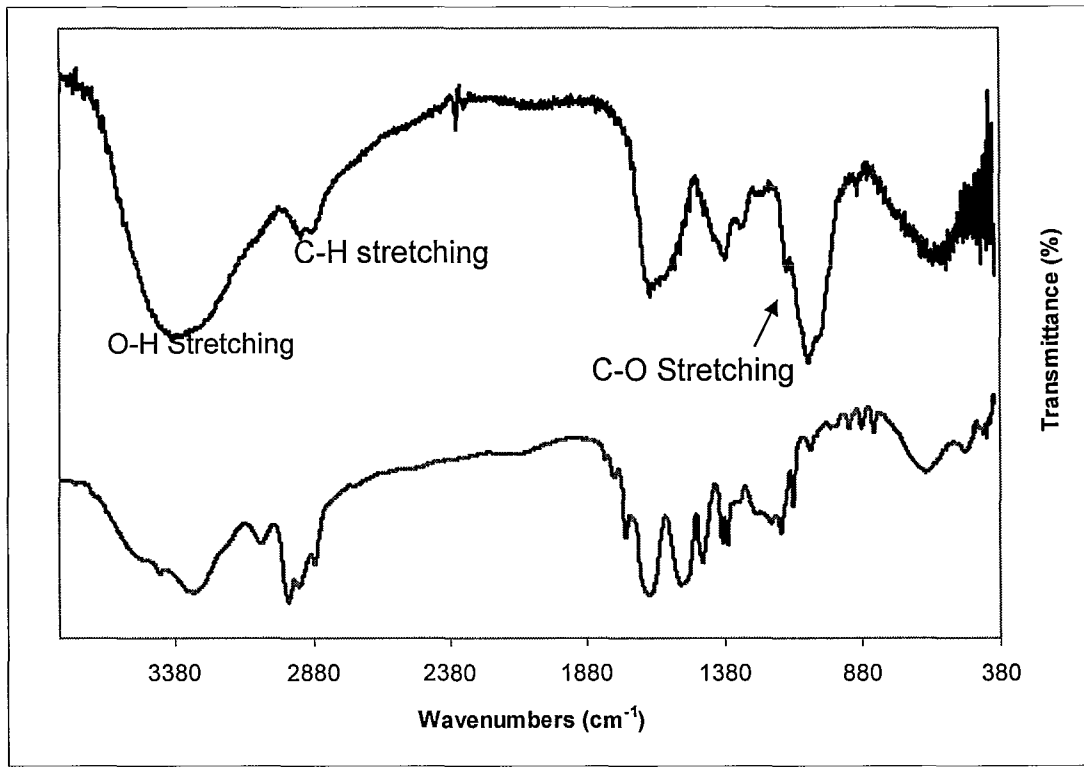

Figure 5-3: FT-IR spectrum of degraded chitosan (top) and CS-P(NIPAM-co-AA) (bottom).

The characteristic peaks of HA were at 1615 cm^{-1} and 1410 cm^{-1} representing asymmetric COO- stretching vibration and symmetric COO- stretching vibration, respectively. The grafting of HA to CS-P(NIPAM-co-AA) was confirm by the overlap of COO- stretching bands of HA with those of CS-P(NIPAM-co-AA).

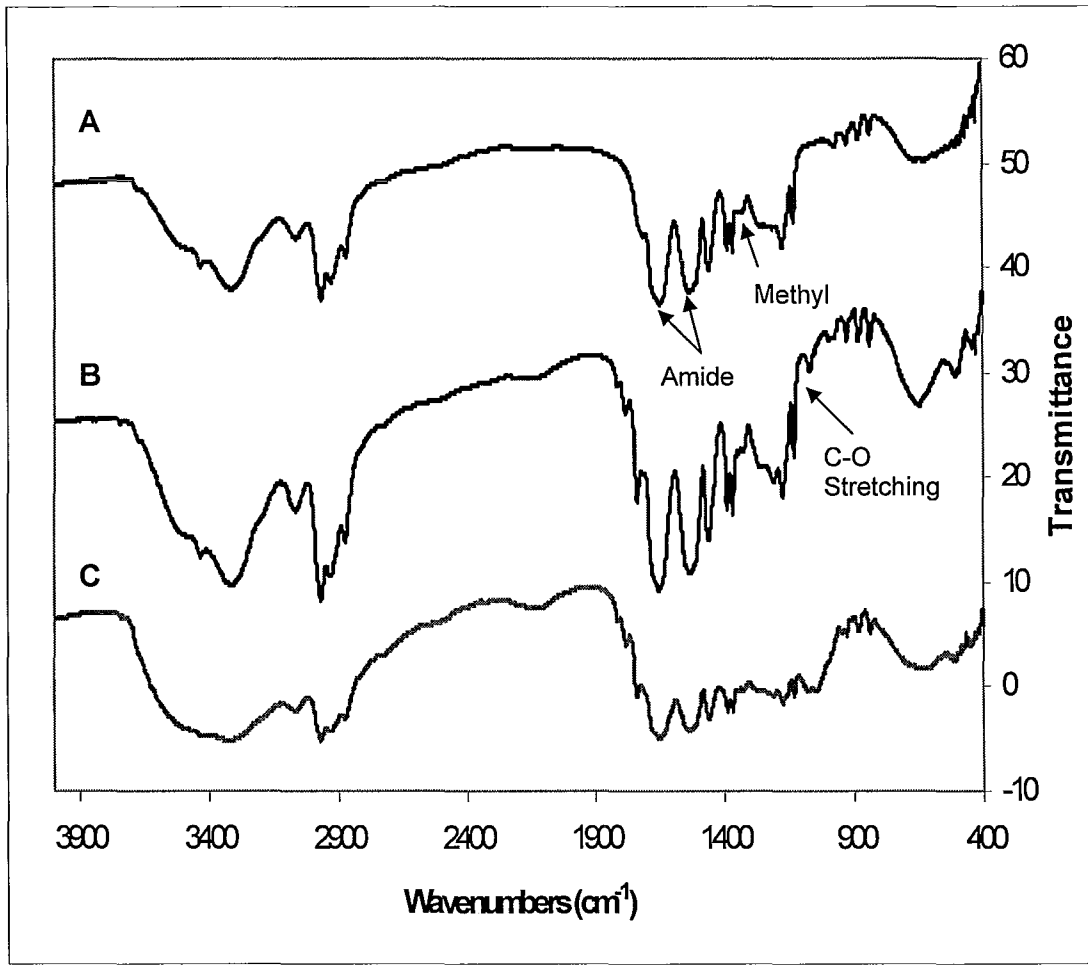

Figure 5-4: FT-IR Spectrum of A: P(NIPAM-co-AA), B: CS-P(NIPAM-co-AA), and C: HA-CS-P(NIPAM-co-AA).

The sol-gel transition behaviour of P(NIPAM-co-AA) was affected by copolymer size and by the fraction of acrylic acid to NIPAM [20, 55]. The size of P(NIPAM-co-AA) was controlled via varying the feed ratio of NIPAM to MAA [53]. The average number molecular weight (Mn) of P(NIPAM-co-AA) copolymers was determined from titration (PC-Titrate^{TM}, Man-Tech) against sodium hydroxide

using acrylic acid to NIPAM fraction obtained from ^{1}H NMR. Although the Mn of sample 2 was higher than that of sample 3 (Table 5-1), the lower critical solution temperature and critical concentration were high in sample 2 due to higher content of the hydrophilic acrylic acid. Increasing Mn of P(NIPAM-co-AA) from 2 kD to 2.5 kD reduced CGC by 40%.

Longer P(NIPAM-co-AA) copolymer 4, was considerably less viscous at room temperature compared to copolymer 3. Copolymer solutions with high viscosity could not be injected via small, 25-30.5 gauge needles. This observation is very important for non-invasive drug delivery and tissue engineering applications.

^{1}H NMR spectra for CS-P(NIPAM-co-AA) and HA-CS-P(NIPAM-co-AA) were used merely to confirm grafting of chitosan and HA, respectively. Grafting ratio could not be determined from ^{1}H NMR due to overlap of peaks and low grafting ratio. However, the characteristic peaks for chitosan and HA were undoubtedly detected between 2.5-3.5 ppm.

In contrast to HA, grafting chitosan to P(NIPAM-co-AA) did not have any noticeable effect on CGC. The CGC of HA-CS-P(NIPAM-co-AA) was 12.5% lower than that of P(NIPAM-co-AA). This large decrease in CGC of HA-CS-P(NIPAM-co-AA) is due to HA contribution to sol-gel transition. HA is known for its ability to hold large amounts of water. Reacting P(NIPAM-co-AA), chitosan, and HA, results in a random polymeric network rather than a grafted polymer network because each polymer contains more than one functional group per

chain.

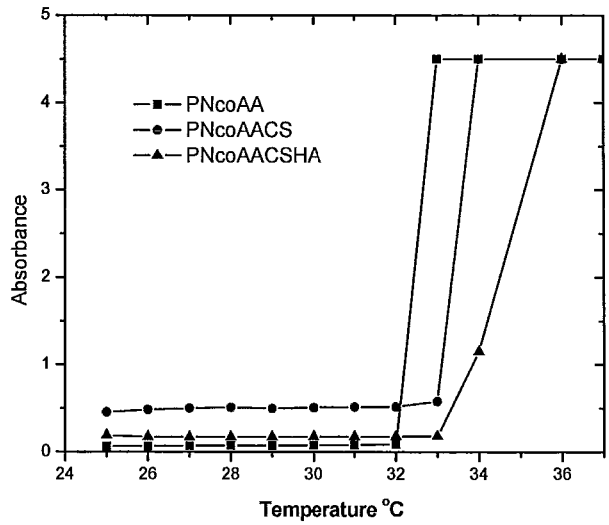

Figure 5-5: Phase transition behaviour of P(NIPAM-co-AA), CS-P(NIPAM-co-AA), and HA-CS-P(NIPAM-co-AA).

The 0.1 mol% chitosan to P(NIPAM-co-AA) in CS-P(NIPAM-co-AA), as determined by TNBS reactions, was enough to increase LCST by 1 °C (from 32 °C to 33 °C) (Figure 5-5). HA incorporation into CS-P(NIPAM-co-AA) increased LCST to 35 °C. Compared to P(NIPAM-co-AA) and CS-P(NIPAM-co-AA), HA-CS-P(NIPAM-co-AA) exhibited a broad phase transition, an indication of reduced thermosensitivity. These findings were expected due to the hydrophilic nature of chitosan and HA.

For the LCST of PNIPAM based hydrogels to be maintained below physiological temperature, the size of the polymer must be balanced with the type and amount of added components. Prior to grafting the component of

interest, the LCST of PNIPAM can be lowered by increasing its MW, yet the reactivity of the polymer decreases due to the lower ratio of functional groups. The optimum size for PNIPAM should allow for enough grafting of other polymer(s) of interest such that biocompatibility and the desired properties are obtained in the final PNIPAM based biomaterial.

Our results indicate that the optimum size of P(NIPAM-co-AA) is in the range of 2-2.5 KDa. In this range, sufficient functional groups were available for chitosan grafting while maintaining the LCST below body temperature. Since HA is known to have better biocompatibility compared to chitosan, utilizing lower molecular weight (degraded) chitosan achieves this goal by providing more space for HA.

The SEM images, shown in Figure 5-6, of polymeric solutions reveal their microstructure details. SEM images show similar microstructure details when images were obtained from samples at critical concentration. Reducing sample concentration resulted in the formation of larger and less uniform pore-sizes. More importantly, reducing copolymer solution concentration reduced the thickness of the separations between the pores, which is an indication of weaker structure (Figure 5-7). Porous materials are desired in biomedical applications to facilitate the biological component, e.g. nutrition, waste, and proteins. In tissue engineering applications, porous biomaterials are required to provide rigid support for cells.

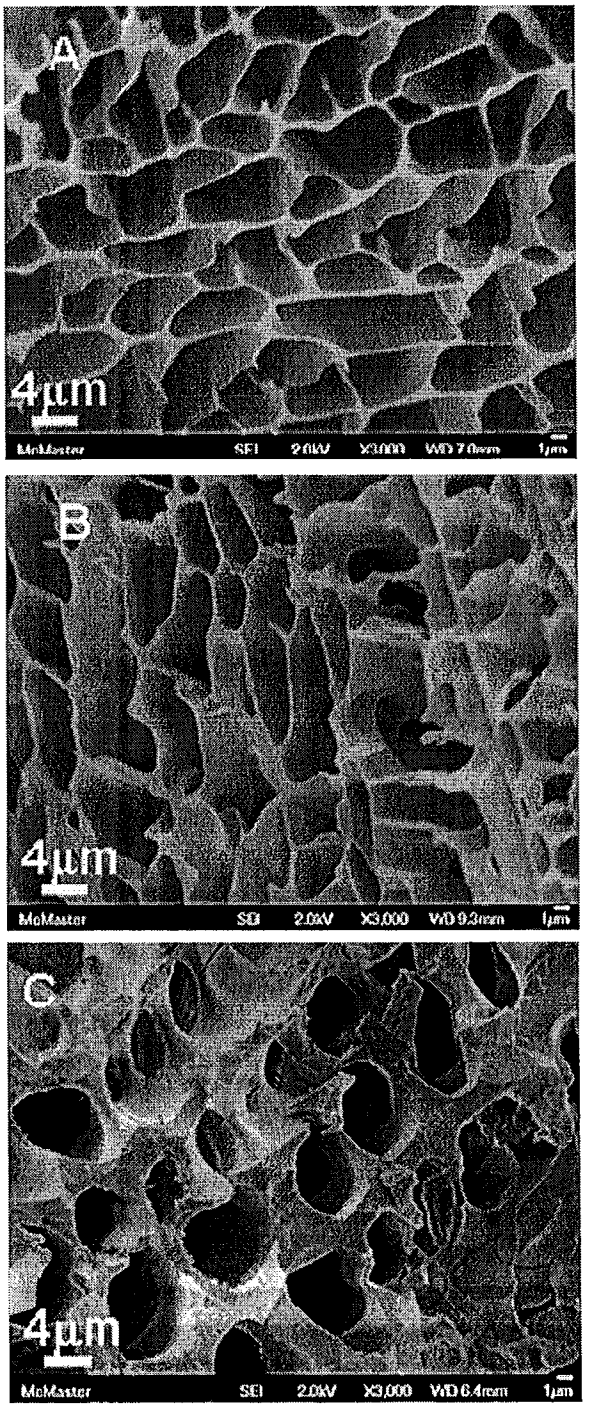

Figure 5-6: SEM images of A: P(NIPAM-co-AA), B: CS-P(NIPAM-co-AA), and C: HA-CS-P(NIPAM-co-AA). Magnification 3,000x.

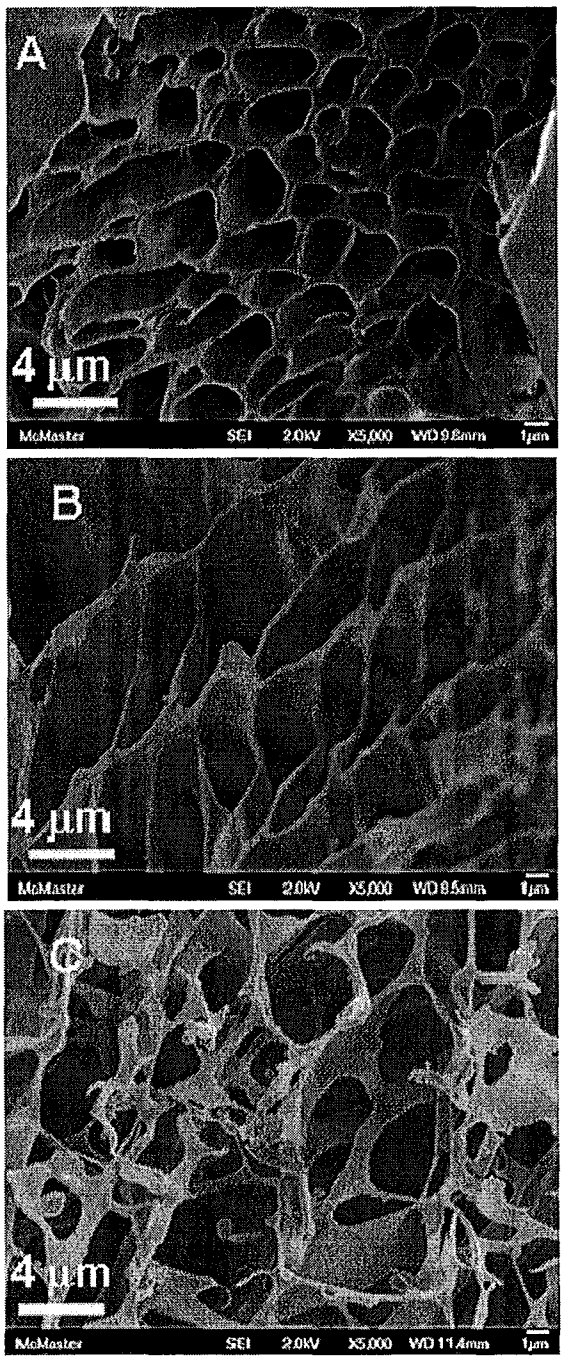

Figure 5-7: SEM images showing effect of concentration of same sample on pore size and size distribution. Images A, B, and C are at concentrations of 20%, 10%, and 5% of CS-P(NIPAM-co-AA) solution, respectively. Magnification 5,000x.

5.3.2. Protein Adsorption

Plasma proteins, such as IgG and C3, are the antigen recognition components of the immune system. IgG mediates adhesion and activation of leukocytes though binding to Fc receptors. Other plasma proteins, such as fibrinogen, C3b, and coagulation factor X, mediate leukocyte adhesion and activation via Mac-1 (CD11b/CD18) receptors on leukocytes. Fibrinogen, fibronectin, and vitronectin are referred to as "adhesive proteins" due to their role in mediating cell adhesion and migration [13, 18, 31].

The type of protein adsorbed to PNIPAM based hydrogels was determined by SDS-page and Western blot experiments presents the results obtained in Figure 5-8. P(NIPAM-co-AA) supported adsorption of all six proteins selected. The incorporation of chitosan to P(NIPAM-co-AA) inhibited C3 adsorption, but only reduced fibrinogen, fibronectin, and vitronectin adsorption. HA incorporation, however, inhibited adhesive adsorption of protein C3 and reduced IgG adsorption. Albumin, which serves as a passivating protein, was clearly present in all surfaces. The effect of HA on inhibiting inflammatory protein adsorption serves as the first indication of significantly reduced inflammatory responses.

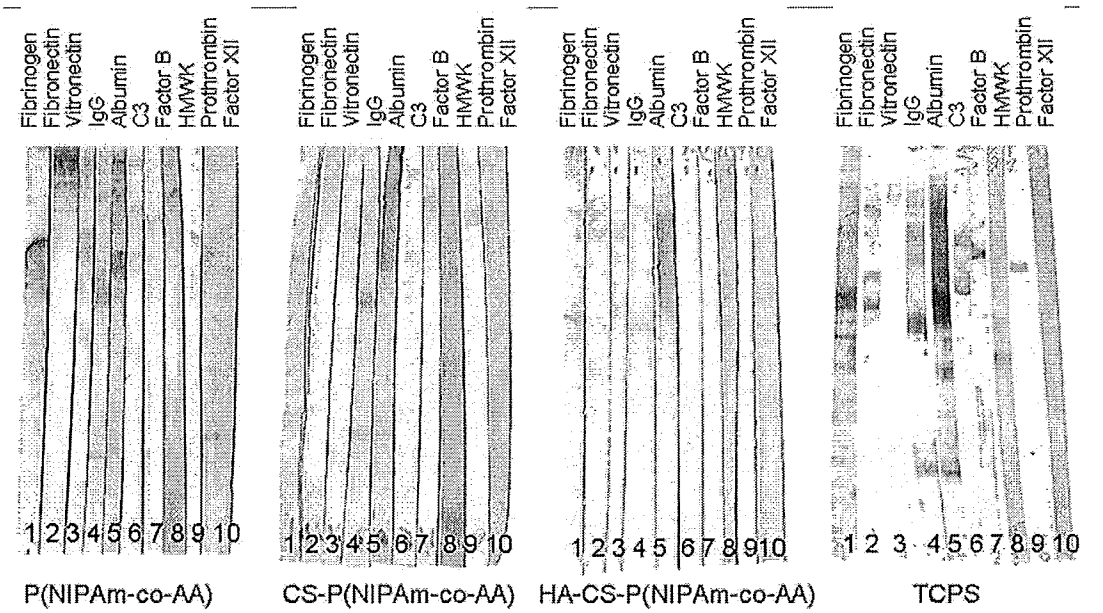

Figure 5-8: Western blots of adsorbed proteins. Surfaces were incubated in plasma and eluted with 2% SDS.

Table 5-3: Protein adsorption to surfaces.

	Protein	P(N-co-AA)	P(N-co-AA)-CS	P(N-co-AA)-CS-HA
1	**Fibrinogen**	X	XL	
2	**Fibronectin**	X	XL	
3	**Vitronectin**	X	XL	
4	**IgG**	X	X	XL
5	**Albumin**	X	X	X
6	**C3**	X		

X: band detected; XL: Light band

5.3.3. *In vitro* Assays

Monocytes/macrophages mediate host responses to implanted biomaterials though the release of cytokines. The levels of pro-inflammatory TNF-α, IL-6, and IL-4, and anti-inflammatory IL-10 were determined over a course of ten days of culture using ELISA kits [76, 80]. IL-6, which plays an important role in mediating both innate and adaptive immunity, was only released by macrophages adherent to P(NIPAM-co-AA) and TCPS. IL-4, IL-10, and TNF-α release was certainly chemistry dependant (Figure 5-9). Grafting chitosan to P(NIPAM-co-AA) reduced the amount of TNF- α release notably compared to P(NIPAM-co-AA) alone. IL-10 production was initially (day 1) higher on P(NIPAM-co-AA) surfaces, but was much higher on chitosan grafted and CS-HA grafted surfaces on days 7 and 10. Monitoring the levels of IL-4 secretion demonstrates that the tendency to form FBGC was not consistent over time. Cytokine release overall proves that grafting chitosan improves the biocompatibility of P(NIPAM-co-AA), which is further improved by grafting HA.

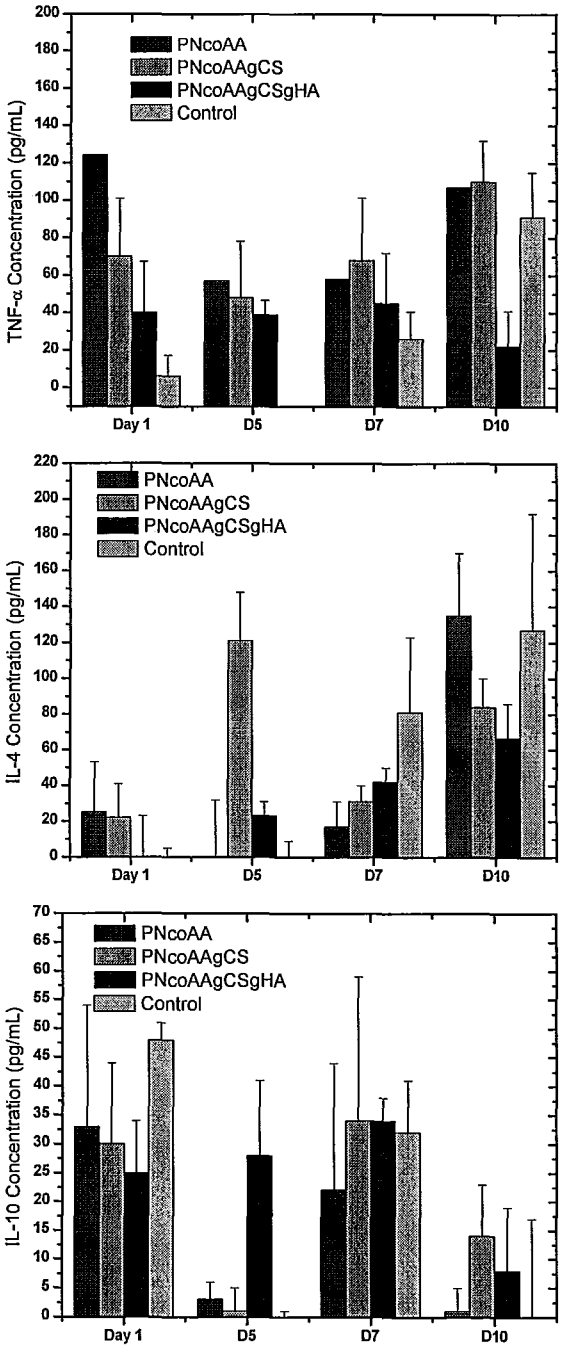

Figure 5-9: Cytokines (TNF-α, IL-4, IL-10) release by blood derived monocytes/lymphocytes cultured on PNIPAM based surfaces. Error bars represent standard deviation.

In contrast to the study of IL-4 release, adherent cell morphology reveals highest percent of macrophage fusion occurs on HA-CS-P(NIPAM-co-AA), followed by P(NIPAM-co-AA), followed by TCPS, although CS-P(NIPAM-co-AA) adherent macrophages were larger in size when compared to macrophages on all other surfaces. This inconsistency could be explained by higher levels of dead cells on P(NIPAM-co-AA) (Figure 5-10). Live/dead assay results denote that P(NIPAM-co-AA) modification decreases apoptosis. Furthermore, Figure 5-11 shows that adherent cell density was significantly lower on modified chitosan grafted P(NIPAM-co-AA) and even less on HA grafted CS-P(NIPAM-co-AA). Adherent cell density results are summarized in Figure 5-12.

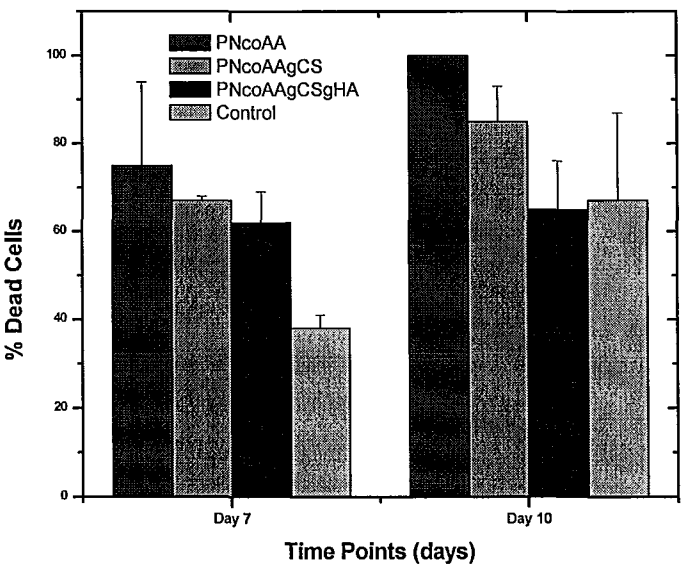

Figure 5-10: Percent dead cells obtained by live/dead fluorescence labelling of leukocyte in the supernatant of TCPS, P(NIPAM-co-AA), CS-P(NIPAM-co-AA), and HA-CS-P(NIPAM-co-AA). Error bars represent standard deviation.

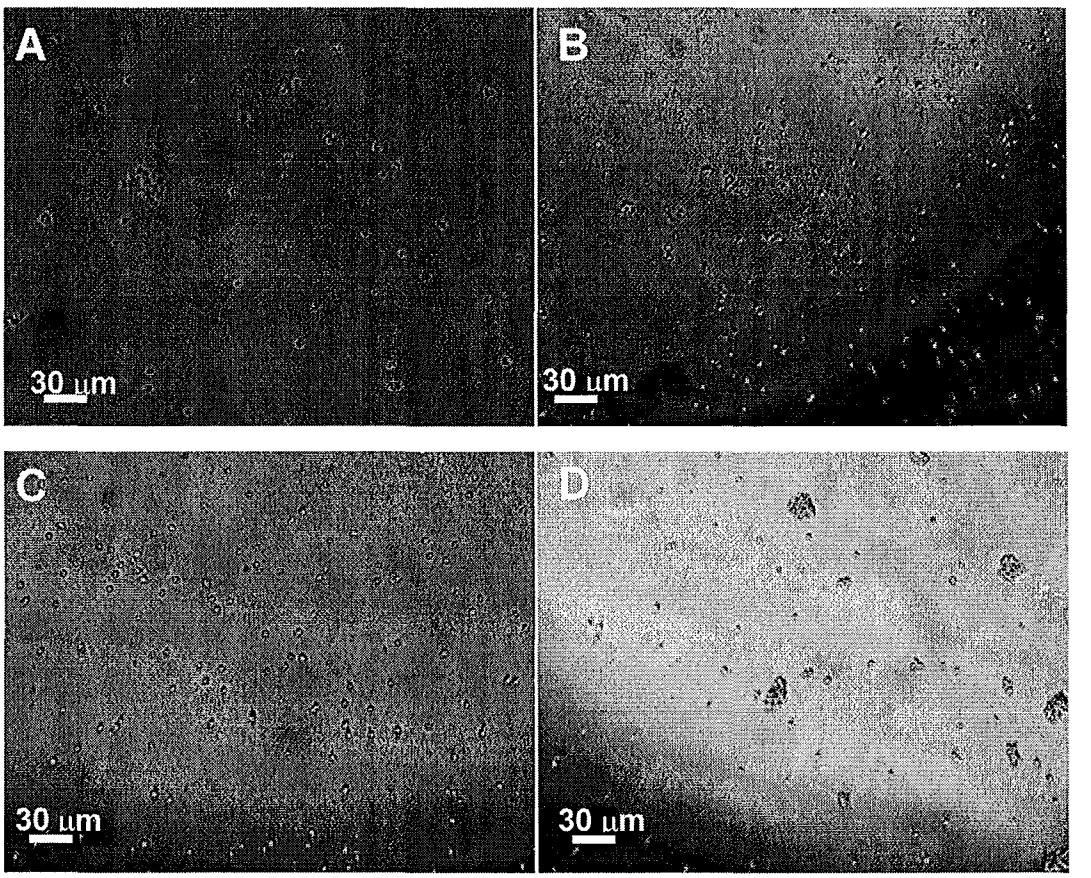

Figure 5-11: Light micrograph of adherent cells. Adherent cells 7 days after culture were collected from PNIPAM based samples by dissolving in excess media at room T. A: control, B: P(NIPAM-co-AA), C: CS-P(NIPAM-co-AA), and D: HA-CS-P(NIPAM-co-AA).

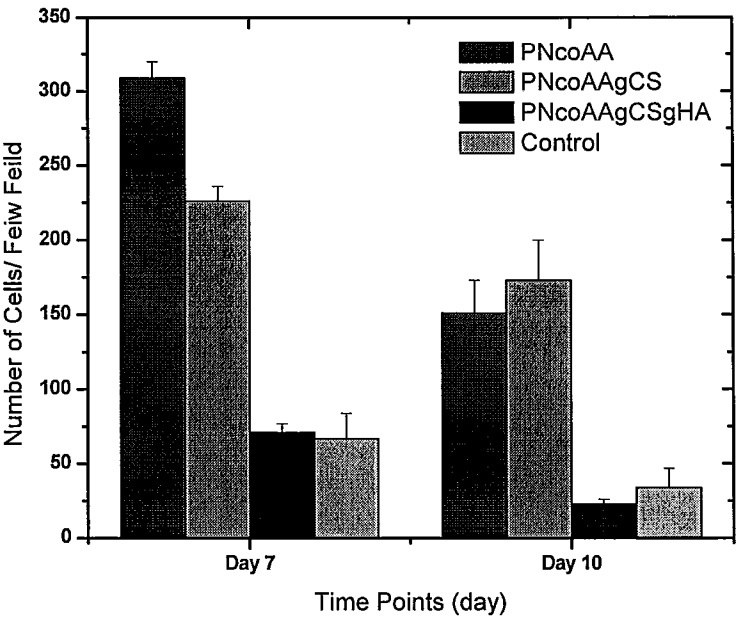

Figure 5-12: Adherent cell density. Blood-derived monocytes/lymphocytes seeded at a density of $3.7x10^5$ cell/well. View field of 20x magnification. Error bars represent standard deviation.

5.3.4. *In vivo* Assays

The dorsal site of injection was shaved and wiped with alcohol to observe the sol-gel transition behaviour of samples *in vivo*. Implants turned white, as shown in Figure 5-13, within one minute post injection, but the protuberance disappeared gradually within half hour. Examining the implant one hour post injection revealed reduction in size, likely due to the liquid uptake by capillaries. The injection site was examined histological at different time points. Careful examination of the injection site indicated that the implant was stationary.

The extent of foreign body reactions was assessed by the extent and

duration of each reaction phase (acute inflammation, chronic inflammation, and FBGCs) and by the up-normality in the overall tissue appearance compared to saline-injected controls [32, 128]. Observing the implant site one day post injection revealed stronger inflammatory reactions to P(NIPAM-co-AA) compared to HA-CS-P(NIPAM-co-AA), as shown in Figure 5-14. Moreover, compared to CS-P(NIPAM-co-AA) and HA-CS-P(NIPAM-co-AA), P(NIPAM-co-AA) induced longer acute inflammation characterized by persistence of neutrophils four days post injection. The formation of connective tissue and presence of monocytes, macrophages, and lymphocytes on P(NIPAM-co-AA) at day four is an indication of phase switch to chronic inflammation.

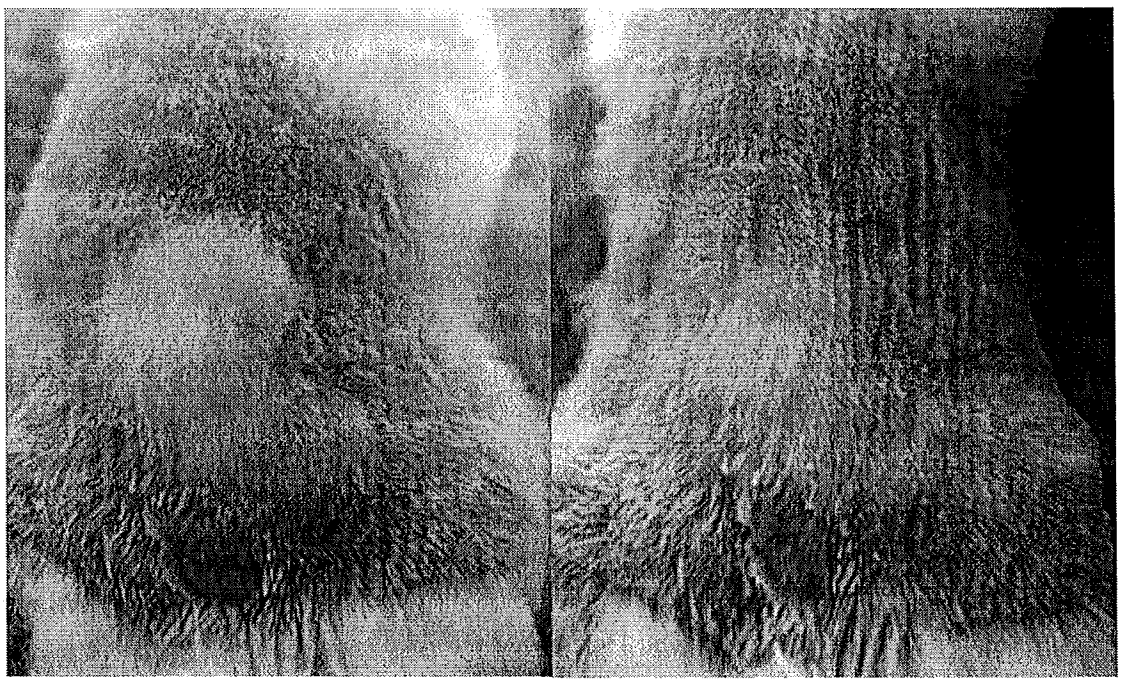

Figure 5-13: *In vivo* phase transition of PNIPAM based solutions. Left image: five minutes post injection. Right image: 30 minutes post injection.

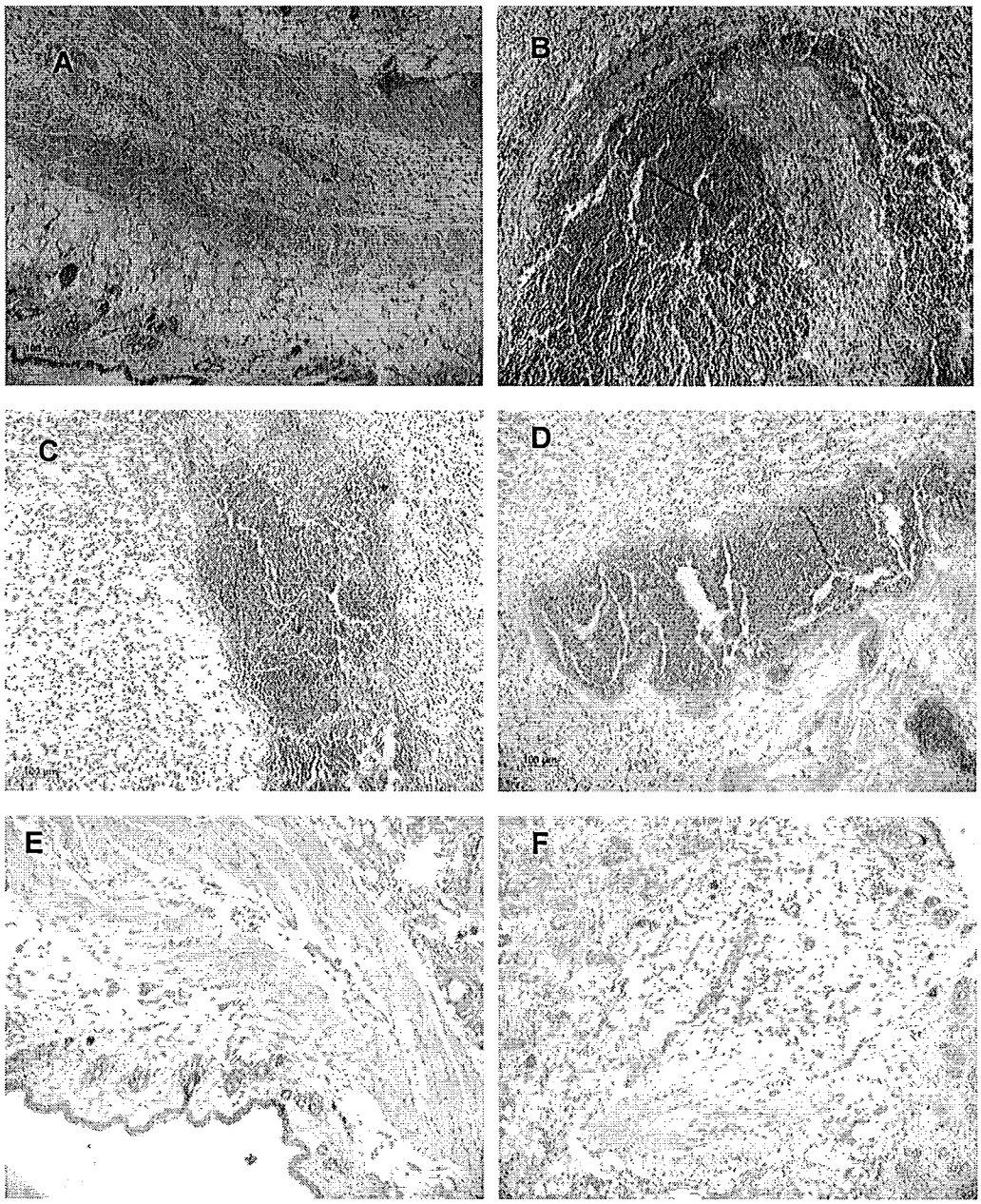

Figure 5-14: Light micrographs showing injection-site sections stained with hematoxylin and eosin at 10x magnification. Images A, B and C are one day post injection of saline, P(NIPAM-co-AA), and CS-P(NIPAM-co-AA), respectively. Images D, E and F are four days post injection of P(NIPAM-co-AA), CS-P(NIPAM-co-AA), and HA-CS-P(NIPAM-co-AA), respectively.

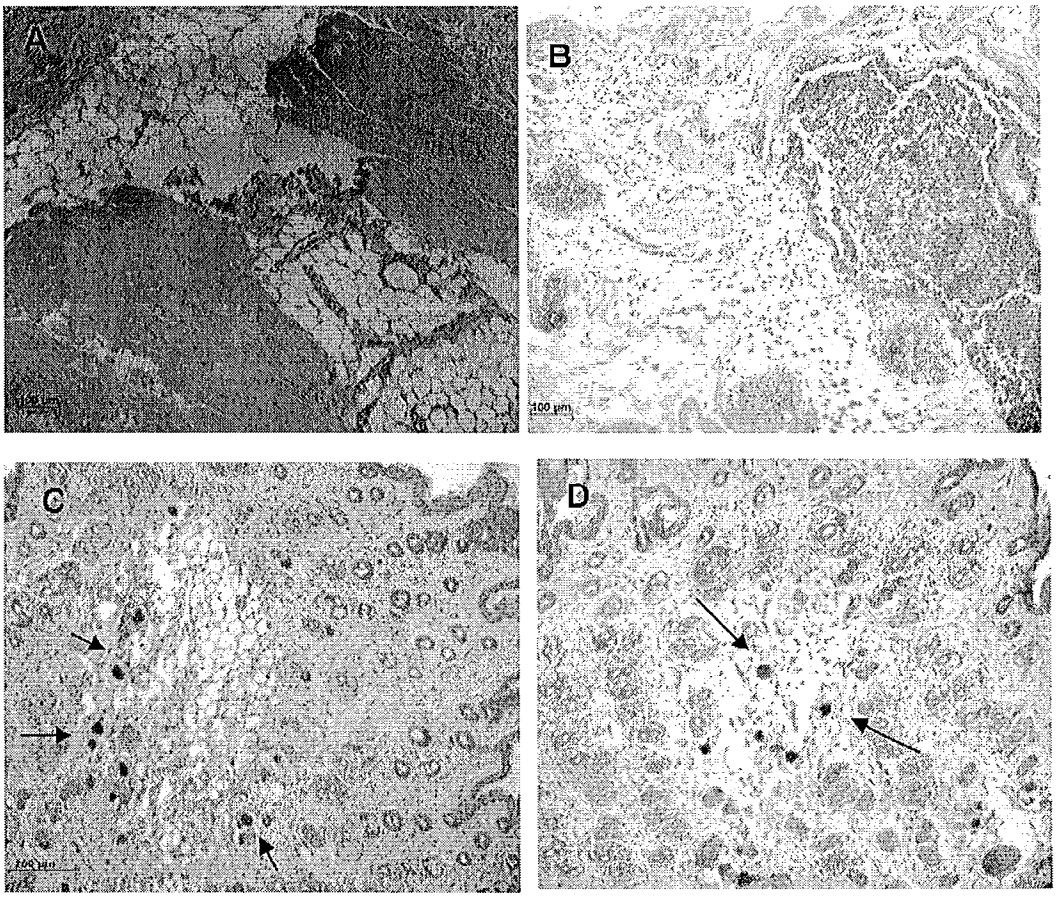

Figure 5-15: Light micrograph of injection-site sections stained with hematoxylin and eosin at 10x magnification. A shows saline one day post injection. B, C and D show P(NIPAM-co-AA), CS-P(NIPAM-co-AA), and HA-CS-P(NIPAM-co-AA), respectively, four days post injection. The arrows indicate FBGCs.

No sites of acute or chronic inflammation were detected on either CS-P(NIPAM-co-AA) or HA-CS-P(NIPAM-co-AA), while granulation tissue, neovascularization, and FBGCs were observed on both samples. Incorporating CS and HA reduced the formation of FBGCs by 60% compared to the incorporation of CS alone (Figure 5-15). It is clear from the observed differences

in the hypodermis layer (subcutaneous tissue) of sham-control, compared to CS-P(NIPAM-co-AA) and HA-CS-P(NIPAM-co-AA), that the implants were not degraded. Thus, grafting chitosan and HA to P(NIPAM-co-AA) speeds the healing process significantly.

5.4. Discussion

5.4.1. Synthesis and Characterization

PNIPAM based injectable systems were synthesized and characterized. The reaction conditions for the preparation of P(NIPAM-co-AA) were optimum size and acrylic acid content that would allow to graft sufficient amounts of chitosan and HA to improve its *in vivo* performance while maintaining transition temperature below body temperature. Consistent with published results, we showed that P(NIPAM-co-AA) of low molecular weights or high AA content exhibited LCST but did not form gel [55]. Han C.K and Bae Y. H. reported that low MW PNIPAM and P(NIPAM-co-AA) prepared in 1,4-doxane exhibit only one transition phase, the LCST phase, while the higher MW samples that were prepared in benzene exhibited three phase transition stages: (i) LCST; (ii) gel formation; and, (iii) shrunken gel formation [20]. The two additional stages were present in benzene samples because longer MW PNIPAM and P(NIPAM-co-AA) chains with lower AA content remain in the random coil conformation when

chitosan chains with lower MW precipitate. Increasing the temperature above the cloud point results in entanglement of longer chains and aggregation of precipitated PNIPAM chains.

Reducing the acrylic acid content from 3 to 1.7 mol % made it possible to observe the gel phase, although the MW was slightly decreased and it required high concentrations of co-polymer (60% w/v). In addition, the solution formed was so viscous that it was not possible to inject it using 25-30' gage needles. Increasing the MW of P(NIPAM-co-AA) to 2,583 while keeping the AA content relatively constant resulted in decreasing CGC from 60% to 20%, making it possible to inject the polymeric solutions using a small needle. Increasing the MW of P(NIPAM-co-AA) by further reducing the molar ratio of MAA/NIPAM would reduce reactivity to chitosan. Degraded soluble chitosan was grafted to P(NIPAM-co-AA) by conjugating the amino groups of chitosan with the carboxylic groups of P(NIPAM-co-AA) utilizing EDC/NHS zero-length crosslinking.

HA and chitosan grafting were confirmed by ^{1}H NMR, FT-IR, change in LCST, and TNBS reactions. It was observed that reducing the ratio of NHS/EDC resulted in lower graft yield of chitosan to P(NIPAM-co-AA). This was not consistent with what was observed in crosslinking gelatin, where 1/5 ratio was reported to yield highest crosslinking [129]. It should be mentioned that only one paper was published on the effect of EDC/NHS ratio on reaction yield. It is very likely that differences in reaction condition and nature of reactive components are responsible for this inconsistency.

The minimal effect of chitosan grafting on the LCST and CGC of P(NIPAM-co-AA) was not expected, although was noted by other groups [25]. This was likely due to comparable hydrophilicity of the two polymers. The CGC of HA-CS-P(NIPAM-co-AA) was 12.5% lower than that of P(NIPAM-co-AA). This large decrease in CGC is due to the hydrophilicity of HA and its ability to hold large amounts of water [62]. It is well documented that incorporating hydrophilic components into PNIPAM increases its LCST [12, 21, 55]. The more hydrophilic the polymer and the higher the composition, the higher the LCST shift. HA incorporation to CS-P(NIPAM-co-AA) increased LCST to 35°C. It is clear that this is the highest amount of HA that could be grafted to CS-P(NIPAM-co-AA) before the sample loses its injectable characteristics.

SEM images revealed porous microstructure details that were dependent on concentration and material. For the same mean pore size, a lower HA-CS-PNIPAM concentration was used compared to P(NIPAM-co-AA) and CS-P(NIPAM-co-AA). This is due to the added water retention ability of HA compared to that of P(NIPAM-co-AA), which was also observed by LCST measurements. The porous microstructure morphology of all samples was similar at their CGC concentrations. The concentration dependent variation in mean pore size for the same sample is indicative of concentration dependent mechanical strength.

5.4.2. Immune Reactions

5.4.2.1. Cell Culture Techniques

Although injectable biomaterials provide interesting advantages when applicable, such as ease of application, localization, and non-invasiveness, many challenges are confronted when running *in vitro* and *in vivo* experiments. Qualitative and quantitative analysis of protein adsorption allows for speculating on the nature and extent of interactions between cells and biomaterials. Biomaterial induced leukocyte activation is evaluated on the basis of adherent cell density, cytokine release, apoptosis, cells differentiation and proliferation, and macrophage fusion density [8, 10, 109]. All of these experiments require stable substrates that closely mimic the actual biomaterials. The temperature-dependent instability of PNIPAM-based or temperature-sensitive biomaterials makes it difficult to obtain accurate results. In this work, we developed techniques that address these issues.

Surfaces were prepared in their shrunken gel form by dissolving the polymeric samples in PBS, such that solution concentrations are above CGC, followed by incubation at 37 °C. All media solutions and reagents used were pre-heated to 40 °C prior to being added to surfaces. Cell-culture plates containing gels were placed on a heating pad and a heating lamp was used to avoid surface erosion. To evaluate adherent cell density and morphology, the supernatant was

removed from cell-culture plates and excess fresh cold media was added to dissolve the polymeric samples. The dissociated cells were then centrifuged and seeded on TCPS plates for microscopic evaluations.

5.4.2.2. Protein Adsorption

Due to the important role they play in mediating cell adhesion and activation, fibrinogen, fibronectin, vitronectin, IgG, albumin, and complement C3 were selected as model proteins in protein adsorption analysis [7]. P(NIPAM-co-AA) supported adsorption of all types of proteins. This was expected because of the hydrophobic nature of PNIPAM above LCST [34]. The incorporation of chitosan to P(NIPAM-co-AA) reduced the amount of most adsorbed inflammatory proteins. Although this indicates that incorporating chitosan improved the biocompatibility of the injectable PNIPAM-based system, it is likely that resultant gel will still fail to avoid foreign body immune responses.

HA-CS-P(NIPAM-co-AA) showed desirable surface properties that inhibited the adsorption of almost all inflammatory proteins. Incorporating non-fouling property through grafting HA has been the goal for many researchers in this area [13, 34, 40, 44, 45, 92]. The non-fouling characteristic of HA depends on crosslinking density [16]. Significant amounts of proteins were adsorbed to sulfated-HA (S-HA) and crosslinked-HA (C-HA). This was attributed to the presence of hydrophobic regions on the polymer chains. The fact that protein

adsorption was inhibited on HA-CS-P(NIPAM-co-AA) surfaces demonstrates that the reactions resulted in sufficient crosslinking. Alternatively, it is possible that protein adsorption was only reduced. Western blotting provides little quantitative measure. The low surface energy and large exclusion volume of their fully hydrated states enable polysaccharides to resist protein adsorption. *In vivo* experiments would determine whether HA-CS-P(NIPAM-co-AA) inhibited or reduced protein adsorption.

5.4.2.3. Mononuclear Cell Activation

The vast majority of *in vitro* evaluations of biomaterials induced immune responses utilize monocytes or macrophages only culture systems [106, 107]. Anderson's group has demonstrated the role lymphocytes play in mediating inflammation through indirect interactions with lymphocytes [35, 100, 103]. For example, macrophages fusion to form FBGCs results from lymphocytes secretion of IL-4. Therefore, a co-culture system of monocytes and lymphocytes was employed in this study. Cell activation was measured through quantification of TNF-α, IL-4, IL-6, and IL-10 release using ELISA kits.

Cytokine release was consistent with protein adsorption, cell adhesion, and live/dead assays. Cytokine release revealed the highest inflammatory reactions on P(NIPAM-co-AA) surfaces and lowest on HA-CS-P(NIPAM-co-AA) surfaces. IL-6 was only secreted by macrophages adherent to P(NIPAM-co-AA)

and TCPS. This suggests more severe and/or longer inflammatory reactions on these surfaces. The higher levels of TNF-α secreted by macrophages adherent to CS-P(NIPAM-co-AA) suggests a possible phenotypic switch when comparing the density of adherent cells on the two surfaces. However, live/dead assay proved no phenotypic switch; apoptosis was not higher on CS-P(NIPAM-co-AA) surfaces compared to P(NIPAM-co-AA) surfaces. No phenotypic switch was observed on either surface throughout the 10-day culture period, but cells were dying by day 7.

5.4.2.4. *In Vivo* Host Response

Placing biomaterials *in vivo*, whether through injection, insertion, or surgical implantation, results in various degrees of tissue injury that turns on wound healing processes [1, 7]. The presence of foreign materials at wound site results in nonspecific immune reactions leading to fibrous capsule formation. The extent of immune reactions is evaluated based on the severity and duration of each of the two inflammatory stages and the thickness of fibrotic tissue that encapsulates the implant [1, 7, 40, 114]. Histological analysis of the injection site showed severe inflammation induced by P(NIPAM-co-AA). Chitosan and chitosan-HA grafting to P(NIPAM-c-AA) significantly improved its biocompatibility. Acute inflammation was resolved by day 3 on both surfaces, but with fewer FBGCs on HA-CS-P(NIPAM-co-AA) compared to CS-P(NIPAM-co-AA).

Compared to the five days to two weeks of acute inflammation present with other hydrogel-based biomaterials, these results prove to be very promising.

Morphological details contribute to biomaterials whether used for drug delivery or tissue engineering applications through affecting active component release and interfacial cells interactions [3, 40, 42, 104, 130]. Examining materials of various pore sizes showed a healing response very similar to normal wound healing associated with materials with pore size in the range of 5-15 μm [41]. The response was independent of the type of material. Our three samples exhibited similar mean pore sizes in CGC. It can therefore be deduced that the porosity of materials did not contribute to the variation observed in immune responses. Additionally, since the mean pore size was above the reported range whereby inflammation is inhibited, the improved biocompatibility was due to material physical and chemical properties rather than morphological properties.

The variation in pore size, pore size-distribution, and interconnectivity suggests that controllable solute exchange, release of active components, and cell behaviour are possible using these biomaterials by varying graft-polymer concentrations [3, 40, 104, 131]. The concentration dependent mechanical properties were evident through the increase in pore mean size and decrease of pore-wall thickness with decreasing graft-polymer concentrations.

5.5. Conclusions

We report P(NIPAM-co-AA), CS-P(NIPAM-co-AA), and HA-CS-P(NIPAM-co-AA) synthesis and characterization. The optimum MW for P(NIPAM-co-AA) that could provide sufficient amount of reactive sites while maintaining LCST below body temperature was found to be in the range of 2-2.5KDa. The hydrophilic nature of chitosan and HA is responsible for the increased LCST observed upon grafting these two polymers to P(NIPAM-co-AA). The hydrogel characteristic of coupled HA contributed to GCG and resulted in 10% reduction compared to P(NIPAM-co-AA) and CS-P(NIPAM-co-AA).

Grafting chitosan to P(NIPAM-co-AA) reduced most inflammatory protein adsorption, and inhibited C3 adsorption. Grafting HA to CS-P(NIPAM-co-AA) almost inhibited inflammatory proteins, despite the low amounts of IgG detected. These results have been confirmed with *in vitro* results that demonstrated reduced inflammation induced by CS-P(NIPAM-co-AA) and HA-CS-P(NIPAM-co-AA) compared to P(NIPAM-co-AA) surfaces. Furthermore, histological analysis of injection sites reveal accelerated healing rate attributed to formation of granulation tissue by day four post injection in chitosan-grafted and chitosan-grafted-HA grafted surfaces.

5.6. Acknowledgements

This project was funded by CHRP. We thankfully acknowledge Allison Fox-Robichaud's group for training on animal handling and Jonh Brash's group for help with protein adsorption analysis.

6. Conclusions

The success of tissue engineering, gene therapy, and drug delivery systems is only possible with the advancement of biomaterials research. This work contributes to biomaterials research field through: i) presenting our results on optimum reaction conditions for the synthesis of important class of biomaterial, ii) proposing a strategy for performing *in vitro* and *in vivo* assays with temperature sensitive hydrogels, and iii) by evaluating immune response to three of the most widely studied polymers in the biomedical field.

7. References

1. Ratner, B.D. and S.J. Bryant, *BIOMATERIALS: Where We have Been and Where we are going* Annu. Rev. Biomed. Eng. , 2004. **6**: p. 41-75.
2. Nair, L.S. and C.T. Laurencin, *Biodegradable polymers as biomaterials* Prog. Polym. Sci. , 2007. **32**: p. 762-798.
3. Castner, D.G. and B.D. Ratner, *Biomedical surface science: Foundations to frontiers* Surface Science, 2001. **500**: p. 28-60.
4. Han, S.-o., et al., *Development of Biomaterials for Gene Therapy.* Molecular Therapy 2000. **2**(4): p. 302-317.
5. Brown, D.M., *Drug Delivery Systems in Cancer Therapy*, ed. D.M. Brown. 2004.
6. Williams, D.F., *On the mechanisms of biocompatibility* Biomaterials, 2008. **29**: p. 2941-2953.
7. Ratner, B.D., et al., *Biomaterials Science: An Introduction to Materials in Medicine* ed. s. Edition. 2006.
8. Anderson, J.M., A. Rodriguez, and D.T. Chang, *Foreign body reaction to biomaterials.* Seminars in Immunology 2008. **20**: p. 68-100.
9. Roach, P., D. Eglin, and K. rohde, *Modern biomaterials: a review- bulk properties and implications of surface modifications* J Mater Sci: Mater Med, 2007. **18**(1263-1277).
10. Anderson, J.M., *BIOLOGICAL RESPONSES TO MATERIALS* Annu. Rev. Mater. Res. , 2001. **31**: p. 81-110.
11. Babensee, J.E., et al., *Host Response to tissue engineered devices.* Advanced Drug Delivery Reviews 1998. **33**: p. 111-139.
12. Qui, Y. and K. Park, *Environment-sensitive hydrogels for drug delivery* Advanced Drug Delivery Reviews, 2001. **53**(2001): p. 321-339.
13. Horbett, T.A. and J.L. Brash, *Proteins at interfaces: current issues and*

future prospects. In proteins at interfaces, 1987. **343**: p. 1-33.

14. Lee, K.Y. and D.J. Mooney, *Hydrogels for Tissue Engineering* Chemical Reviews, 2001. **101**(7): p. 1869-1879.
15. Klouda, L. and A.G. Mikos, *Thermoresponsive hydrogels in biomedical applications* European Journal of Pharmaceutics and Biopharmaceutics 2008. **68**: p. 34-45.
16. Phillips, G.O., J.J. Kennedy, and P.A. Williams, *Hyaluronan* 2002.
17. Liu, Y., X. Shu, and G. Prestwich, *Biocompatibility and stability of disulfide-crosslinked hyaluronan films* Biomaterials, 2005. **26**(4737-4746).
18. Lord, M.S., et al., *Protein adsorption on derivatives of hyaluronic acid and subsequent cellular response.* Journal of Biomedical Materials Reserach Part A 2008: p. 636-646.
19. De Souza, R., et al., *Biocompatibility of injectable chitosan-phospholipid implant system* Biomaterials, 2009. **30**: p. 3818-3824.
20. Han, C.K. and Y.H. Bae, *Inverse thermally-reversible gelation of aqueous N-isopropylacrylamide copolymer solutions* Polymer, 1998. **39**(13): p. 2809-2814.
21. Jeong, B., S.W. Kim, and Y.H. Bae, *Thermosensitive sol-gel reversible hydrogels* Advanced Drug Delivery Reviews, 2002 **54**: p. 37-51.
22. Stile, R.A., W.R. Burghardt, and K.E. Healy, *Synthesis and Characterization of Injectable Poly(N-isopropylacrylamide)-Based hydrogels That Support Tissue FOrmation in Vitro* Macromolecules 1999. **32**: p. 7370-7379.
23. Chen, J.-P. and T.-H. Chen, *Functionalized temerature-sensitive copolymer for tissue engineering of articular cartilage and meniscus* Colloids and surfaces A: Physiochem. Eng. Aspects, 2007. **313-314**: p. 254-259.
24. Chen, J.-P. and T.-H. Chen, *Preparation and evaluation of thermo-reversible copolymer hydrogels containing chitosan and hyaluronic acid as*

injectable cell carriers Polymer, 2009. **50**: p. 107-116.

25. Chen, J.-P. and T.-H. Cheng, *Thermo-Responsive Chitosan-grafted-poly(N-isopropylacrylamide) Injectable Hydrogel for Cultivation of Chondrocytes and Meniscus Cells* Macromolecular Bioscience, 2006. **6**(6): p. 1026-1039.
26. Ottenbrite, R.M. and S.W. Kim, *Polymeric drugs & drug delivery systems* 2000.
27. Bonadio, J., S.A. Goldstein, and R.J. Levy, *Gene therapy for tissue repair and regeneration* Advanced Drug Delivery Reviews, 1998. **33**: p. 53-69.
28. Zhou, H.-s., D.-p. Liu, and C.-c. Liang, *Challenges and Strategies: The Immune Responses in Gene Therapy* Medicinal Research Reviews, 2004. **24**(6): p. 748-761.
29. Butterfield, A., *Biofunctional membranes*. 1995.
30. Brodbeck, W.G., et al., *Biomaterial Surface Chemistry Dictates Adherent Monocyte/Macrophage cytokine Expression in Vitro.* Cytokine, 2002. **18**(6): p. 311-319.
31. Kao, W.J., J.A. Hubbell, and J.M. Anderson, *Protein-mediated macrophage adhesion and activaton on biomaterials: a model for modulating cell behavior.* Journal of Materials scicence: Materials in medicine, 1999. **10**: p. 601-605.
32. Barbosa, J.N. and A.P. Aguas, *The influence of functional groups of self-assembled monolayers on firbrous capsule formation and cell recruitment* J Biomed Mater Res A, 2005. **76**(4): p. 737-743.
33. A., H.T. and B.J. L., *Proteins at interfaces: current issues and future prospects* in *Protein at Interfaces*. 1987.
34. Horbett, T.A. and J.L. Brash, *Protein at interfaces: an overview* in *Proteins at Interfaces II: Fundamentals and Applications,* . 1995. p. 1-25.
35. MacEwan, M.R. and J.M. Anderson, *Monocyte/lymphocyte interactions and foreign body response: in vitro effects of biomaterial surface chemistry*

Journal of biomedical materials research 2005. **74A**(3): p. 285-293.

36. Recum, V. and J.E. Jacobi, *Handbook of Biomaterials Evaluation: scientific, technical, and clinical testing of implant materials*, ed. n. edition. 1999.
37. al, S.e., *The Development of a Tissue-Engineered Cornea: Biomaterials and Culture Methods.* Cornea Tissue Engineering Methods 2008. **63**(5): p. 535-544.
38. Ma, P.X. and J. Elisseef, *Scaffolding in Tissue Engineering* 2006.
39. Sanders, J.E., C.E. Stiles, and C.L. Hayes, *Tissue response to single polymer fibers of varying diameters: evaluation of fibrous encapsulation and macrophage density.* J. Biomed. Mater. Res., 2000. **52**: p. 231-237.
40. Ratner, B.D., *Reducing capsular thickness and enhancing angiogensis around implant drug release systems.* Journal of Controlled Release 2002. **78**: p. 211-218.
41. Brauker, J.H., et al., *Neovascularization of synthetic membranes directed by membrane microarchitecture* J. Biomed Mater Res., 1995. **29**: p. 1516-1524.
42. Karp, R.D., et al., *Tumorigenesis by Millipore filters in mice: Histology and ultrastructure of tissue reactions as related to pore size.* J. Natl Cancer INst. , 1973. **51**(4): p. 1275-1279.
43. Sharkway, A.A., et al., *Engineering the tissue which encapsulates subcutaneous implants. I. Diffusion properties.* J. Biomed Mater Res., 1997. **37**: p. 401-412.
44. Hoffman, A.S., *Hydrogels for biomedical applications* Advanced Drug Delivery Reviews, 2002. **43**: p. 3-12.
45. Bryant, B.D.R.a.S.J., *Biomaterials: Where We Have Been and Where We Are Going.* Annu. Rev. Biomed. Eng., 2004. **6**: p. 41-75.
46. Klouda, L. and A.G. Mikos, *Thermoresponsive hydrogels in biomedical applicatoins.* European Journal of Pharmaceutics and Biopharmaceutics,

2008. **68**(2008): p. 34-45.

47. E, P., *Biodegradable polymers as biomaterials.* Journal of Biomaterials Science-Polymer Edition, 1995. **6**(9): p. 775-795.
48. MP, L. and H. JA, *Synthetic biomaterials as instructive extracellular microenvironments for morphogenesis in tissue engineering.* Nature Biotechnology, 2005. **23**(1): p. 47-55.
49. Schild, H.G., *POLY(N-ISOPROPYLACRYLAMIDE): EXPERIMENT, THEORY AND APPLICATION.* Prog Polym. Sci., 1992. **17**(163-249).
50. Chen, J.-P. and T.-H. Cheng, *Functionalized temperature-sensitive copolymer for tissue engineering of articular cartilage and meniscus.* Colloids and surfaces A: Physiochem. Eng. Aspects, 2008. **313-314**: p. 254-259.
51. Hoare, T. and R. Pelton, *Highly pH and Temperature Responsive Microgels Functionalized with Vinylacetic Acid.* Macromolecules, 2004. **37**: p. 2544-2550.
52. Ishifune, M., et al., *Polymerization of Acrylamide in Aqueous Solution of Poly(N-isopropylacrylamide) at Lower Critical Solution Temperature.* Journal of Macromolecular Science Part A: Pure and Applied Chemistry, 2008. **45**(523-528).
53. Dincer, S., A. Tuncel, and E. Piskin, *A potential Gene Delivery Vector: N-Isopropylacrylamide-ethyleneimine* Macromolecular Chemistry and Physics 2002. **203**: p. 1460-1465.
54. Tan, H., et al., *Thermosensitive injectable hyaluronic acid hydrogel for adipose* Biomaterials, 2009. **30**: p. 6844-6853.
55. Yoo, M.K., et al., *Effect of polyelectrolyte on the lower critical solution temperature of poly(N-isopropyl acrylamide) in the poly(NIPAAm-co-acrylic acid) hydrogel* Polymer, 2000. **41**: p. 5713-5719.
56. Sugimoto, M. and Y. Shigemasa, *Preparation and characteriation of water-soluble chitin and chitosan derivatives.* Carbohydrate Polymers,

1998. **36**: p. 49-59.

57. Kim, K.H., J. Kim, and W.H. Jo, *Preparation of hydrogel nanoparticles by atom transfer radical polymerization of N-isopropylacrylamide in aqueous media using PEG macro-initiator* Polymer, 2005. **46**(9): p. 2836-2840.
58. Ha, D.I., et al., *Preparation of Thermo-Responsive and Injectable Hydrogels Based on Hyaluronic Acid and Poly(N-isopropylacrylamide) and Their Drug Release Behaviors.* Macromolecular Research, 2006. **14**(No. 1): p. 87-93.
59. Ohnishi, H. and Y. Machida, *Biodegradation and distribution of water-soluble chitosan in mice.* Biomaterials, 1999. **20**: p. 175-182.
60. Tian, F., et al., *The depolymerization mechanism of chitosan by hydrogen peroxide.* Journal of Materials Science 2003. **38**: p. 4709-4712.
61. Kim, I.-Y. and C.-S. Cho, *Chitosan and its derivatives for tissue engineering applications.* Biotechnology Advances, 2008. **26**(1-21).
62. Allison, D.D. and J. Grande-Allen, *Review. Hyaluronan: A Powerful Tissue Engineering Tool.* Tissue Engineering, 2006. **12**(No. 8): p. 2131-2142.
63. Kogan, G., et al., *Hyaluronic acid: a natural biopolymer with a broad range of biomedical and industrial applications.* Biotechnol Lett, 2007. **29**: p. 17-25.
64. Bartolazzi, A., et al., *Glycosylation of CD44 Is Implicated in CD44-mediated Cell Adhesion to Hyaluronan.* The Journal of Cell Biology, 1996. **132**(No. 6): p. 1199-1208.
65. Schade, U., et al., *Hyaluronate and its receptors in bone marrow.* Acta histochemica, 2006. **108**: p. 141-147.
66. Lesley, J., et al., *CD44 in inflammation and metastasis* Glycoconjugate Journal, 1997. **14**: p. 611-622.
67. al, S.e., *Differential involvement of the hyaluornan (HA) receptors CD44 and receptor for HA-mediated motility in endothelial cell function and angiogensis* J Biol chem, 2001. **276**(36770-26778).

68. Chen, J. and G. Abatangelo, *Wound Repair and Regeneration.* 1999. **7**(79089).

69. Kobayashi, H., Americal Journal of Physiology 1997. **276**(C1151-1159).

70. R., J.S. and J. A., *Glutaraldehyde crosslinked chitosan as a long acting biodegradable drug delivery vehicle: studies on the in vitro release of mitoxantrone and in vivo degradation of microspheres in rats muscle* Biomaterials, 1995. **16**: p. 769-775.

71. S., P., et al., *Characterization of porous collagen/hyaluronic acid scaffold modified by 1-ethyl-3-(3-dimethylaminopropyl)carbodiimide cross-linking* Biomaterials, 2002. **23**: p. 1205-1212.

72. K.P., V., et al., *Synthesis and in vitro degradation of new polyvalent hydrazide cross-linked hydrogels of hyaluronic acid.* Bioconjugate Chem., 1997. **8**: p. 686-694.

73. Moller, S., et al., *Dextran and hyaluronan methacrylate based hydrogels as matrices for soft tissue reconstruction* Biomolecular Engineering 2007. **24**: p. 496-504.

74. A., M., et al., *Two-step elution of human serum proteins from different glass-modified surfaces: A comparative proteomic analysis of adsorption patterns* Electrophoresis, 2004. **25**: p. 2413-2424.

75. Leach, J.B., et al., *Photocrosslinked Hyaluronic Acid Hydrogels: Natural, Biodegradable Tissue Engineering Scaffolds.* Biotechnology and Bioengineering, 2002. **82**(No. 5): p. 578-589.

76. Abbas, A.K. and A.H. Lichtman, *Cellular and Molecular Immunology* ed. F. Edition. 2005.

77. McNally, A.K. and J.M. Anderson, *Complement C3 Participation in monocyte adhesion to different surfaces* Proc. Natl. Acad. Sci USA, 1994. **91**: p. 10119-10123.

78. Nilsson, B. and J.D. Lambris, *The role of complmenet in biomaterial-indced inflammation.* Molecular Immunology 2007. **44**: p. 82-94.

79. Smith, M.J. and G.L. Bowlin, *In vitro evaluations of innate and acquired immune responses to electrospun polydioxanon-elastin blends.* Biomaterials, 2009. **30**: p. 149-159.
80. Jones, J.A. and J.M. Anderson, *Proteomic analysis and quantification of cytokines and chemokines from biomaterial surface-adherent macrophage and foreign body giant cells.* Journal of Biomedical Materials Reserach Part A, 2006(585-596).
81. Khan, M.M., *Immunopharmacology* 2008.
82. Schindler, L.W., *Understanding the Immune System.* 1991.
83. Derkins, S., *The Immune System.* 2001.
84. S., L., P. I., and V. JP, *Tissue engineering and its potential impact on surgery.* World Journal of Surgery, 2001. **25**(1): p. 1458-1466.
85. A., A., *Tissue engineering, stem cells and cloning: current concepts and changing trends.* Expert Opinion on Biological Therapy, 2005. **5**(7): p. 879-892.
86. JM, C., et al., *Biomaterials for Blood-Contacting Applications.* Biomaterials, 1994. **15**(10): p. 737-744.
87. Zia, Z. and J.T. Triffitt, *A review on macrophage responses to biomaterials.* Biomed. Mater I 2006. **1**(No. 1): p. R1-R9.
88. A., B., et al., *Pverexpression of a hydrogen peroxide-resistant periplasmic Cu, Zn, superoxide dismutase protects Escherichia coli from macrophage killing.* Biochem. Biophys. Res. , 1998. **243**: p. 804-7.
89. L., B., et al., *Nitric oxide and cell viability in inflammatory cells: a role for NO in macrophage function and fate* Toxicology, 2005. **208**: p. 249-58.
90. Bridges, A.W., et al., *Reduced acute inflammatory responses to microgel conformal coatings.* Biomaterials, 2008. **29**: p. 4605-4615.
91. McNally, A.K. and J.M. Anderson, *Complement C3 participation in monocyte adhesion to different surfaces.* Proc. Natl. Acad. Sci USA, 1994. **91**: p. 10119-23.

92. Miller, J.M.A.a.K.M., *Biomaterial Biocompatibility and the macrophage.* Biomaterials, 1984. **5**: p. 5-10.

93. Ziats, N.P., K.M. Miller, and J.M. Anderson, *In vitro and in vivo interactions of cells with biomaterials.* Biomaterials, 1988. **9**: p. 5-13.

94. McNally, A.K. and J.M. Anderson, *Interleukin-4 Induces Foreign Body Giant Cells from Human Monocytes/Macrophages.* American Journal of Pathology 1995. **147**(No. 5): p. 1487-1499.

95. Jenny, C.R. and J.M. Anderson, *Alkylsilane-modified surfaces: Inhibition of human macrophage adhesion and foreign body giant cell formation.* J Biomed Mater Res 1999. **46**(1): p. 11-21.

96. Kao, W.J., J.A. Hubbell, and J.M. Anderson, *Protein-mediated macrophage adhesion and activation on biomaterials: a model for modulating cell behavior.* Journal of Materials Scicence: Materials in Medicine, 1999. **10**(601-605).

97. Collier, T.O. and J.M. Anderson, *Protein and surface effects on monocyte and macrophage adhesion, maturation, and survival.* J. Biomed Mater Res., 2001. **60**(3): p. 487-96.

98. McNally, A.K. and J.M. Anderson, *Foreign Body-Type Multinucleated Giant Cell Formation Is Potently Induced by α-Tocopherol and Prevented by Diacylglycerol Kinase Inhibitor* American Journal of Pathology, 2003. **163**(No. 3): p. 1147-1156.

99. Collier, T.O., et al., *Inhibition of macrophage development and foreign body giant cell formation by hydrophilic interpenetrating polymer network.* J Biomed Mater Res A 2004. **69**(4): p. 644-50.

100. Brodbeck, W.G., et al., *Lymphocytes and the foreign body response : Lymphocyte enhancement of macrophage adhesion and fusion.* Journal of biomedical materials research, 2005. **74A**(No. 2): p. 222-229.

101. MacEwan, M.R., et al., *Monocyte/lymphocyte interactions and the foreign body response: in vitro effects of biomaterial surface chemisty* Journal of

biomedical materials research Part A, 2005. **74A**(3): p. 285-293.

102. J.A., J., et al., *Instability of self-assembled monolayers as a model material system for macrophage/FBGC cellular behavior.* J Biomed Mater Res A, 2008. **86**(1): p. 261-8.
103. D.T, C., et al., *Lymphocyte/macrophage interactions: biomaterial surface-dependent cytokine, chemokine, and matrix protein production.* J Biomed Mater Res A, 2008. **87**(3): p. 676-87.
104. Cao, H., et al., *The topographical effect of electrospun nanofibrous scaffold on the in vivo and in vitro foreign body reaction* J biomed Mater Res A, 2009. **93**(3): p. 1151-9.
105. A., R. and J.M. Anderson, *Evaluation of clinical biomaterial surface effects on T lymphocyte activation.* J biomed Mater Res A, 2010. **92**(1): p. 214-20.
106. SB, O., et al., *Activation of human mononuclear cells by porcine biologic meshes in vitro.* Hernia, 2010. **14**(4): p. 401-407.
107. MJ, S., et al., *Modulation of murine innate and acquired immune responses following in vitro exposure to eletrospun blends of collagen and polydioxanone.* Journal of biomedical materials research Part A, 2010. **93A**(2): p. 793-806.
108. Khang, D., et al., *Reduced responses of macrophages on nanomter surface features of altered alumina crystalline phases.* Acta Biomaterialia, 2009. **5**(5): p. 1425-1432.
109. Anderson, J.M. and J.A. Jones, *Phenotypic dichotomies in the foreign body reaction* Biomaterials, 2007. **28**: p. 5114-5120.
110. Cadee, J.A., et al., *In vivo biocompatibility of dextran-based hydrogels.* J Biomed Mater Res, *2000.* **50**(No. 3): p. 397-404.
111. Stevens, K.R., et al., *In vivo biocompatibility of gelatin-based hydrogels and interpenetrating networks* J. Biomater. Scie. Polymer Edn, 2002. **13**(No. 12): p. 1353-1366.

112. Pereira, I.H.L., et al., *Photopolymerizable and injectable polyurethanes for biomedical applications: Synthesis and biocompatibility* Acta Biomaterialia, 2010. **6**(3056-3066).
113. Allen, L.T., et al., *Surface-induced changes in protein adsorption and implications for cellular phenotypic responses to surface interaction* Biomaterials, 2006. **27**: p. 3096-3108.
114. Brdiges, A.W. and A.J. Garcia, *Chronic inflammation responses to microgel-based implant coatings.* Journal of Biomedical Materials Reserach Part A, 2009: p. 252-258.
115. Jofuji, K., et al., *Therapeutic effecacy of sustained drug release from chitosan gel on local inflammation.* International Journal of Pharmaceutics, 2004. **272**: p. 65-78.
116. Zhu, C., et al., *Initial investigation of novel human-like collagen/chitosan scaffold for vascular tissue engineering.* Journal of biomedical materials research Part A, 2009. **89**(3): p. 829-40.
117. Tomihata, K. and Y. Ikada, *In vitro and in vivo degradation of films of chitin an dits deacetylated derivatives.* Biomaterials, 1997. **18**: p. 567-575.
118. Souza, R.D., et al., *Biocompatibility of injectable chitosan-phospholipid implant systems.* Biomaterials, 2009. **30**: p. 3818-3824.
119. Chupa, J.M., et al., *Vascular cell responses to polysaccharide materials: in vitro and in vivo evaluations.* Biomaterials, 2000. **21**: p. 2315-2322.
120. Han, H.D., et al., *Preparation and Biodegradation of Thermosensitive Chitosan Hydrogel as a Function of pH and Temperature.* Macromolecular Research 2004. **12**(No. 5): p. 507-511.
121. Tan, H., et al., *Injectable in situ forming biodegradable chitosan-hyaluronic acid based hydrogels for cartilage tissue engineering.* Biomaterials, 2009. **30**: p. 2499-2506.
122. Kim, I.-Y., et al., *Chitosan and its derivatives for tissue engineering applications.* Biotechnology Advances, 2007. **26**: p. 1-21.

123. Carlson, R.P., et al., *Anti-biofilm properties of chitosan-coated surfaces.* J. Biomater. Scie. Polymer Edn, 2008. **19**(No. 8): p. 1035-1046.

124. Ahmadi, R. and J.D.d. Bruijn, *Biocompatibility and gelation of chitosan-glycerol phosphate hydrogels* J biomed Mater Res Part A, 2007. **86A**(3): p. 824-832.

125. Liu, Y., X.Z. Shu, and G.D. Prestwich, *Biocompatibility and stability of disulfide-crosslinked hyaluronan films.* Biomaterials, 2005. **26**: p. 4737-4746.

126. Cornelius, R.M. and J.L. Brash, *Identification of protein adsorbed to hemodialyser membranes from heparinized plasma* J. Biomater Sci. Polymer Edn., 1993. **4**(3): p. 291-304.

127. Babensee, J.E., et al., *Immunoblot analysis of proteins associated with HEMA-MMA micropasules: Human serum proteins in vitro and rat proteins following implantation.* Biomaterials, 1998. **19**: p. 839-849.

128. Dalu, A. and B. Delclos, *A comparison of the inflammatory response to a polydimethylsiloxane implant in male and female Balb/c mice.* Biomaterials, 2000. **21**: p. 1947-1957.

129. Kuijpers, A.J., et al., *Cross-linking and characterisation of gelatin matrices for biomedical applications.* J. Biomater. Scie. Polymer Edn, 2000. **11**(No. 3): p. 225-243.

130. Hironaka, e.a., *Renal basement membranes by ultrahigh resolution scanning electron microscopy.* Kidney Int, 1993. **43**: p. 334-45.

131. Malafaya, P.B., et al., *Morphology, mechanical characterization and in vivo neo-vascularization of chitosan particle aggregated scaffolds architectures.* Biomaterials, 2008. **29**: p. 3914-3926.